The T3SS structural and effector genes of *Chlamydia trachomatis* are expressed in distinct phenotypic cell forms.

Authors:
Nicole A. Grieshaber*, Cody Appa*, Megan Ward*, Alorah Grossman*, Sean McCormik*, Brendan S. Grieshaber*, Travis Chiarelli*, Hong Yang**, Anders Omsland**, and Scott S. Grieshaber*+

*Department of Biological Sciences, University of Idaho, Moscow, ID
**Allen School for Global Health, Washington State University, Pullman, WA

+ Corresponding Author: Scott S. Grieshaber, scottg@uidaho.edu

Abstract:
Bacteria in the chlamydiales order are obligate intracellular parasites of eukaryotic cells. Within this order, the genus *Chlamydia* contains the causative agents of a number of clinically important infections of humans. Biovars of *C. trachomatis* are the causative agents of trachoma, the leading cause of preventable blindness worldwide, as well as sexually transmitted infections with the potential to cause pelvic inflammatory disease and infertility. Irrespective of the resulting disease, all chlamydial species share the same obligate intracellular life cycle and developmental cell forms. They are reliant on an infectious cycle consisting of at least three phenotypically distinct cell forms termed the reticulate body (RB), the intermediate body (IB) and the elementary body (EB). The EB is infectious but does not replicate. The RB replicates in the host cell but is non-infectious, while the IB is an intermediate form that transitions to the EB form. In this study, we ectopically expressed the transcriptional repressor Euo, the two nucleoid-associated proteins HctA and HctB, and the two component sensor kinase CtcB in the RB. Transcriptional analysis using RNA-seq, differential expression clustering and fluorescence *in situ* hybridization analysis show that the chlamydial developmental cycle is driven by three distinct regulons corresponding to the RB, IB or EB cell forms. Moreover, we show that the genes for the T3SS were cell type restricted, suggesting defined functional roles for the T3SS in specific cell forms.

Importance:
Chlamydia trachomatis, a sexually transmitted bacterial infection, poses a significant global health threat, causing over 100 million infections annually and leading to complications like ectopic pregnancy and infertility. This study investigates the gene expression patterns of *Chlamydia trachomatis* during its unique life cycle within human cells. As an obligate intracellular parasite, *C. trachomatis* transitions through distinct developmental stages - one for infection and dissemination, another for replication, and a third for transitioning back to the infectious form. By analyzing gene expression profiles at each stage, we identified key genes involved in these processes. Interestingly, our research also reveals the presence of two separate T3SS (Type III Secretion System) translocons expressed in distinct stages, suggesting their crucial roles in specific functions during the infection cycle.

Introduction:

Many bacterial species undergo dramatic phenotypic changes to adapt to different environments or to generate cells with specific physiological functions. All the bacteria in the Chlamydiales order are obligate intracellular parasites of eukaryotic cells that undergo a developmental cycle with both non-replicating and actively replicating cell forms [1,2]. Chlamydial species are important pathogens of humans. *C. psittaci* causes zoonotic infections resulting in pneumonia, while *C. pneumoniae* is a human pathogen that causes respiratory disease. Biovars of *C. trachomatis (Ctr)* are the causative agents of trachoma, the leading cause of preventable blindness worldwide, as well as sexually transmitted infections with the potential to cause pelvic inflammatory disease, ectopic pregnancy and infertility [3–5].

Success of a chlamydial infection depends on the completion of a complex intracellular developmental cycle, consisting of multiple cell forms; the elementary body (EB), the reticulate body (RB) and the intermediate body (IB) [1,2]. Although the timing of cell type conversion may differ, the broad strokes of this cycle are conserved in all the Chlamydiaceae [6,7]. Our current understanding of the developmental cycle as determined through promoter reporter strains, single inclusion kinetics, single cell gene expression and agent based modeling has led to a clearer picture of the cycle [8,9]. The EB, characterized by its condensed nucleoid and small size (~0.2 nm diameter), initiates infection of the host through the use of a type III secretion system (T3SS) and pre-formed effectors [10,11]. These effectors promote pathogen phagocytosis and entry into the targeted cell. After entry, the EB form resides in an endocytic vesicle termed the inclusion that is modified through chlamydial gene expression [10,11]. The EB completes EB to RB differentiation and becomes replication competent at ~10 hpi (*Ctr* serovar L2) [12]. The RB, which is phenotypically characterized as larger than the EB (~1 nm diameter) and containing a dispersed nucleoid, then undergoes several rounds of amplifying replication before maturing to produce IB cells that then progress to the infectious EB, a process that takes place over ~8-10 hours after IB formation [8,9]. The mature RBs continue to produce IB cells, acting as a stem cell population [9]. This developmental program results in a growth cycle that does not act like a typical bacterial growth culture (lag, log, stationary phase) but instead asynchronously progresses through the RB, IB and EB cell type transitions until cell lysis or inclusion extrusion [1,2,8,9].

The current understanding of the regulation of the developmental cycle comes primarily from population level studies that frame the cycle in terms of time, treating the chlamydial population as a time dependent uniform culture. Population level gene expression data has been determined for chlamydial infections and has been described according to time after infection. These studies include RT-qPCR, microarray and RNA-seq studies and contribute to the canonical early (~0-10 hpi, EB to RB differentiation), mid-cycle (~10-18 hpi, RB replication) and late (~18 hpi-cell lysis, EB formation) gene expression paradigm [13–16]. The reliance on population level data of a mixed cell population has confounded the understanding of gene expression as it pertains to the specific chlamydial cell forms.

Here we sought to define the transcript profiles of the cell forms that underpin the observed growth cycle by investigating the effects of ectopic expression of four transcriptional regulatory proteins in *Chlamydia trachomatis* (*Ctr*): Euo, HctA, HctB and CtcB. Euo (Early Upstream ORF) is among the earliest genes expressed post EB to RB differentiation during chlamydial infection [17]. Current evidence suggests that Euo is a DNA binding protein that acts to repress a handful of late cycle genes [17,18].

The HctA protein is a small DNA binding protein that is expressed transiently in the IB cell type ~8-10 hrs before HctB [8,9]. HctA has been shown to bind DNA and to repress transcription broadly across chromosomes of both *Ctr* and, when ectopically expressed, *E. coli* [19–21]. HctB is a second small positively charged protein that has limited homology to the H1 histone family and is thought to contribute to condensation of the EB nucleoid [22]. Our data show that unlike HctA, HctB is expressed late in EB development, during the final stages of EB formation [8,9]. In addition to these DNA binding proteins, *Ctr* contains a single cytosolic two component regulatory system (TCS) consisting of CtcB/CtcC (histidine kinase/response regulator) [23]. The *Ctr* TCS is actively transcribed during RB to EB development, and the protein products are functional with respect

to phosphotransfer [23]. Additionally, expression of the ATPase effector domain of the response regulator, CtcC, resulted in the up regulation of the sigma54 regulon which included many developmentally regulated genes [24]. We expect that ectopic expression of CtcB would phosphorylate CtcC and amplify the signaling and activation process of sigma 54 gene expression.

We have shown that Euo, HctA and HctB promoter activities help define the RB, IB and EB cell forms [8,9]. Therefore, along with CtcB we determined the effects of ectopic expression of these regulatory factors on the transcriptome of *Ctr* using RNA-seq. Our data produced gene regulation profiles consistent with cell form-specific transcriptomes. This allowed us to bin the expression of a large fraction of the chlamydial genome into RB, IB and EB-specific transcript categories. Within our cell form expression prediction groups was a number of T3SS genes. Using fluorescence *in situ* hybridization (FISH), we showed that components of the T3SS were expressed in specific cell forms.

Results:

Ectopic expression of Euo, HctA, CtcB, and HctB resulted in disruption of the developmental cycle. To determine the effects of the ectopic expression of Euo, HctA, HctB and CtcB on gene expression and the developmental cycle, we expressed these proteins and the GFP protein Clover as a control from the chlamydial plasmid. We chose to induce expression at 15 hpi in order to evaluate the effects of these proteins on the RB to EB stage of the developmental cycle. At 15 hpi the vast majority of the chlamydial cells would be in the RB form [9].

We expressed each of these constructs in *Ctr* using the native plasmid, the T5 promoter (*E. coli* sigma70 constitutive promoter) and the E riboswitch for conditional translational expression [25]. The ORFs of each of the four transcriptional regulatory proteins (*euo*, *hctA*, *ctcB*, and *hctB*) were cloned upstream of a C-terminal FLAG tag and transformed into *Chlamydia trachomatis* serovar L2 434/bu (*Ctr*) creating the strains L2-E-euo-FLAG, L2-E-hctA-FLAG, and L2-E-ctcB-FLAG. As described previously, we could not successfully transform *Ctr* with the E-hctB-FLAG construct, therefore we developed a tet-riboJ-E promoter system that combines both transcriptional and translational control to hctB-FLAG expression, creating the strain L2-tet-J-E-hctB-FLAG [25].

Cells were infected with each strain and expression of Euo-FLAG, HctA-FLAG, CtcB-FLAG, HctB-FLAG and Clover-FLAG was induced at 15 hpi. We tested for the production of infectious progeny (EBs) using a reinfection assay at 48 hpi. Ectopic expression of all four transcriptional regulatory proteins resulted in a significant inhibition of EB production as compared to the Clover-FLAG controls (Fig. 1A). In addition, infected cells were imaged using transmission electron microscopy (TEM). Cells were infected with L2-E-euo-FLAG, L2-E-hctA-FLAG, L2-E-ctcB-FLAG, L2-tet-J-E-hctB-FLAG and L2-E-clover-FLAG, induced for expression at 15 hpi and fixed and prepared for TEM analysis at 30 hpi (Fig. 1B). The induced and uninduced Clover-FLAG control samples were indistinguishable. The inclusions for both samples had similar ratios of RBs (large cell forms) and EBs (small electron dense forms). Cells ectopically expressing Euo had inclusions with very few visible EBs (small electron dense forms) and most cells appeared RB like (large less electron dense cell forms). In the HctB and HctA expressing bacteria, the inclusions contained few abnormal RB like forms as well as cells with dense structures resembling condensed nucleoids (electron dense regions inside cells). The inclusions of the CtcB expressing bacteria contained both RB and EB-like cells and an increase in intermediate forms, i.e. RB sized cells with condensed nucleoids (Fig. 1B). These data suggested that ectopic expression of all four of these transcriptional regulatory proteins resulted in an aborted developmental cycle as indicated by both the IFU studies and the dysregulated cell forms seen by EM.

RNA-seq of the ectopic protein expressing chlamydial strains. To better understand the effects of the ectopic expression of each regulatory protein, we used RNA-seq to characterize the corresponding transcriptomes. We infected host cells with each strain (L2-E-clover-FLAG, L2-E-euo-FLAG, L2-E-hctA-FLAG

140 L2-E-ctcB-FLAG and L2-tet-J-E-hctB-FLAG), induced expression at 15 hpi and harvested RNA for library
141 construction at 18 hpi and 24 hpi. We chose to investigate gene expression three hours after induction (18 hpi)
142 to capture potential immediate effects on the developmental cycle. We also investigated gene expression at 9
143 hours after induction (24 hpi) as we reasoned that this time point would capture potential effects of inhibition of
144 the advancement of the cycle. This later time point allowed for the detection of changes between the
145 advancement of the cycle in control samples vs potential inhibition of the cycle by ectopic expression of the
146 regulatory proteins.
147 We compared the transcriptome of each sample in triplicate using principal component analysis (PCA).
148 Each of the triplicate samples clustered closely together suggesting little differences between the biological
149 replicates (Fig. 2A). As expected, the Clover control samples clustered in distinct groups depending on
150 isolation timepoint. The 18 hpi samples clustered together in a grouping and the 24 hpi samples clustered in a
151 separate distinct grouping. For the Euo induced samples, all the 18 hpi and 24 hpi samples clustered closely
152 together suggesting only small differences between both the time point samples. The timepoint experimental
153 samples were also clustered together for the HctA 18 hpi and 24 hpi samples. For the HctB 18 hpi and 24 hpi
154 experimental samples, each time point clustered separately but the two clusters were closer to each other than
155 any of the other experimental conditions. The CtcB 18 hpi and 24 hpi experimental samples were similar, the
156 replicates for each time point clustered tightly together and the 18 hpi and 24 hpi samples clustered closer to
157 each other than to the samples from the other experimental conditions.(Fig. 2A). Together, these data suggest
158 that each ectopically expressed protein generated a unique gene expression pattern.
159 The RNA-seq data sets were compared to the induced Clover controls; 18 hpi Clover to 18 hpi
160 experimental sample, and 24 hpi Clover to 24 hpi experimental samples. In addition to the ectopic data, we
161 used the gene expression data from our published data set (NCBI's Sequence Read Archive (SRA),
162 submission number GSE276506) and determined the differential gene expression between *Chlamydia* from
163 the 18 hpi sample and the 24 hpi sample, capturing changes in late gene expression (RB to IB and EB). We
164 compared this differential gene expression pattern to the differential gene expression patterns of the ectopic
165 expression experimental data. We generated a hierarchically-clustered heatmap using the Seaborn clustering
166 algorithm [26] (Fig. 2B and C). The 24 hpi samples for Euo and HctB were used for clustering analysis as these
167 proteins acted as inhibitors and blocked cycle progression (Fig. 2B and C). The 24 hpi samples allowed more
168 time for accumulated changes as the Clover controls progressed to the production of late genes while the Euo
169 and HctB expressing samples did not. The 18 hpi data from the HctA and CtcB ectopic expression experiments
170 were used for cluster analysis as they both acted as inducers (Fig. 2B and C). These changes were most
171 obvious in the 18 hpi samples as the Clover controls had not begun to express late genes.
172 Clustering produced two dominant groups (Fig. 2B and C). Both groups featured genes that were
173 dramatically up-regulated between 18 hpi vs 24 hpi during the wt infection (Fig. 2B and C, HeLa_24h)
174 suggesting that all of these genes would be considered late genes [14,15]. The major difference between the two
175 cluster groups is the changes in gene expression induced by HctA and CtcB ectopic expression (Fig. 2B and
176 C). One of the clusters featured genes that were not dramatically induced upon HctA-FLAG or CtcB-FLAG
177 ectopic expression (Fig. 2B). The other cluster showed the opposite with all the genes upregulated by the
178 ectopic expression of HctA-FLAG and CtcB-FLAG (Fig. 2C). Ectopic expression of Euo-FLAG and HctB-FLAG
179 led to a down-regulation of both of these sets of genes as compared to the Clover control (Fig. 2B and C).
180 Many of the genes in the first cluster (Fig. 2B) have been shown to be expressed mid-cycle or late-cycle [14,15],
181 while most of the genes in the second cluster (Fig. 2C) have been identified to be expressed late in the
182 developmental cycle [14,15]. Additionally, many of the second cluster genes have been identified as
183 sigma54/ctcB-ctcC regulated genes [24,27]. These data suggest that the late expressed genes can be divided into
184 two distinct categories.
185
186 **Gene expression cluster groups map to cell type specific gene expression profiles.** Using the clustering

data observations, we created a selection criteria to categorize the RNA-seq data into three gene expression categories (Table S1). The first group were genes for which we observed little to no change after Euo ectopic expression when compared to the Clover control and had little to no change between 18 hpi and 24 hpi during a wt infection. We separated the late genes into two groups. The first group was defined as genes whose expression increased between 18 hpi and 24 hpi in the wt infection but were not induced by HctA, CtcB or Euo ectopic expression. The second group of late genes were defined as genes whose expression was increased from 18 hpi to 24 hpi in the wt infection and were up-regulated by CtcB and HctA ectopic expression but not increased by Euo ectopic expression. Based on the observation that *euo* was a member of the first group, we defined these genes as RB genes (Table S1). For the two late gene groups we noticed that *hctA*, an IB gene [8,9], was a member of the first group and therefore designated this group as IB genes (Table S1). The second late gene group was designated as EB genes, i.e., the regulon likely involved in the final stage of generating EB infectivity. This group contains the hctB, tarp, and scc2 genes that we have previously shown to be expressed late in the IB to EB developmental stage [8,9].

We next used volcano plots to visualize the individual effects of each of the ectopic expression constructs on changes in gene expression of all *Ctr* genes. The expression changes were plotted (log2fold change) vs statistical significance (-log of the p value) and the RB, IB and EB gene groups designated in Table S1 were highlighted (Fig. 3). We plotted changes in gene expression from 18 hpi to 24 hpi from a wt infection, which as expected indicated that the genes from Table S1 designated as RB genes were largely unchanged in gene expression between 18 hpi and 24 hpi, while both the designated IB and EB genes showed increased expression. RB gene expression was for the most part unchanged when Euo was ectopically expressed in contrast to dramatic reductions in the expression of both IB and EB designated genes (Fig. 3, Euo 24hpi vs Clover 24hpi). The ectopic expression of both HctA and CtcB dramatically increased the expression of EB genes (Fig. 3, HctA and CtcB 18hpi vs Clover 18hpi). HctB ectopic expression also resulted in a dramatic repression in the expression of both IB and EB genes while also increasing the relative expression of a subset of RB genes relative to Clover (Fig. 3, HctB 24hpi vs Clover 24hpiE). We noticed that many of the genes that showed increased expression when HctB was ectopically expressed were ribosomal protein genes (Fig. 3, HctB 24hpi vs Clover 24hpi). We interpreted this effect as HctB inhibiting the expression of most genes with the exception of the ribosomal genes, perhaps allowing them to be expressed early during EB to RB differentiation upon the next infection cycle.

Fluorescence *in situ* hybridization verification of cell type gene expression. To verify the association of binned genes with specific cell forms we used fluorescence *in situ* hybridization (FISH) to visualize gene expression in cells expressing GFP and RFP from developmental stage-specific promoters. To this end, we constructed two dual promoter reporter constructs to delineate gene expression from the *euo*, *hctA* and *hctB* promoters which we have shown to be associated with RB, IB and EB cells forms respectively. We generated the strains L2-*hctB*prom_Scarlet-*euo*prom_neongreen (L2-BsciEng) and L2-*hctA*prom_Scarlet-*euo*prom_neongreen (L2-AsciEng) which express the RFP mScarlet-I (sci) from either the *hctB* promoter or *hctA* promoter along with the GFP protein Neongreen (ng) driven by *euo* promoter. To validate our system, the mRNA expression of *euo*, *hctA* and *hctB* was visualized in each strain using custom FISH probes from Molecular Instruments (Fig. 4). Cells were infected with L2-AsciEng and L2-BsciEng and processed for each FISH probe at 24 hpi. Although dual promoter strains were used in these experiments, the data is presented in a single promoter format to simplify presentation. *Euo* and *hctA* data was processed from L2-AsiEng samples and *hctB* data was processed from L2-BsciEng samples. As expected, *euo* mRNA was observed primarily in the *euo*prom+ (RB) cells and not in either of the *hctA*prom+ (IB) or *hctB*prom+ (EB) cells (Fig. 4A). The *hctA* mRNA was observed in a subset of cells that had overlap with the *hctA*prom signal but not *euo*prom or *hctB*prom signal (Fig. 4B). The *hctB* mRNA was observed in a subset of cells with overlap with *hctA*prom+ and *hctB*prom+ cells but not *euo*prom+ cells (Fig. 4C).

To quantify the FISH results, we used the TrackMate plugin in Fiji [28] to identify and measure both the mRNA signal and promoter reporter signal for each chlamydial cell in five inclusions from each infection. Cells were identified by their promoter reporter signal (green) and separately by their mRNA fluorescence signal (pink). The fluorescence intensity was measured and plotted for both channels (FISH and promoter reporter) in both identified populations. Therefore, each plot represents two identified cell populations per reporter, mRNA+ (pink) population and their corresponding promoter reporter fluorescence intensity, and the promoter reporter+ (green) population and their corresponding FISH signal. This analysis was performed for all three promoter reporters (*euo*p, *hctA*p and *hctB*p) for each FISH mRNA probe (*euo*, *hctA*, and *hctB*) (Fig. 4).

RB: *euo* FISH. Using Fiji and TrackMate, we identified individual chlamydial cells expressing the *euo* mRNA in host cells that were infected with the promoter reporter strains expressing fluorescent proteins from the *euo*prom, *hctA*prom, and *hctB*prom. The analysis indicates that the *euo* mRNA+ cell population (pink) when plotted for *euo*prom fluorescence and *euo* mRNA fluorescence were primarily double positive with high levels of both *euo* FISH signal and *euoprom* signal. These *euo* mRNA+ cells from *hctAprom* infections were primarily single positive. This was also observed for the *hctB*prom infections; the *euo* mRNA+ cells when plotted for *euo* mRNA FISH signal intensity against *hctB*prom signal intensity were primarily single positive (Fig. 4A).

We also used TrackMate to identify the promoter reporter positive cell populations (green) and plotted the expression intensities of the promoter reporter signals against the *euo* mRNA FISH signal. The *euo*prom+ cells were predominantly double positive (high *euo* mRNA signal, high *euo*prom signal), while the *hctA*prom+ cells and *hctB*prom+ cell populations (green) were predominantly single positive (low *euo* mRNA signal high *hctA*prom or *hctB*prom signal) (Fig. 4A).

IB: *hctA* FISH. The *hctA* mRNA positive population was identified in the *euo*prom, *hctA*prom and *hctB*prom infected cells using TrackMate (magenta) and the intensities of the *hctA* mRNA FISH signal was plotted against each of the promoter reporter intensity signals. The *hctA* mRNA+ cells from the *euo*prom infection were mostly single positive but had carryover Neongreen signal from RB *euo*prom expression (Fig. 4B). The *hctA* mRNA+ cell population (magenta) was mostly double positive when compared to the *hctA*prom signal. Additionally, the *hctA* mRNA+ population had little to no *hctB*prom signal (Fig. 4B).

We identified the promoter reporter positive chlamydial cells (green) and plotted both the promoter reporter signals and the FISH signal. The *euo*prom+ cell population (green) was mostly single positive with a small population of double positive cells presumably from the long lived Neongreen protein carry-over (Fig. 4B). The *hctA*prom+ cell population (green) demonstrated a large double positive sub-population as well as a single positive sub-population that again was likely due to the long half-life of the mScarlet-I protein carried over into the EB population (Fig. 4B). The *hctB*prom+ cell population was almost entirely single positive with little *hctA* mRNA signal (Fig. 4B).

EB: *hctB* FISH. We performed the same analysis for the *hctB* mRNA+ cells (magenta). The *hctB* mRNA+ chlamydial cells were mostly single positive when compared to the *euo*prom signal with some detected long-lived *euo*prom signal (Fig. 4C). The *hctB* mRNA+ cells were generally double positive for the *hctA*prom signal and double positive for the *hctB*prom signal (Fig. 4C). For the promoter reporter cells (green), the *euo*prom+ cells had a significant single positive population and a smaller double positive sub-population, while the *hctA*prom+ cells were both single and double positive for the *hctB* mRNA signal. In the *hctB*prom+ cells there was both a single and double positive population (Fig. 4C).

The apparent disconnect between mRNA expression and cognate fluorescent protein fluorescence for euo, hctA and hctB FISH results are as expected as the fluorescent proteins have a much longer half life than mRNA. Additionally, fluorescence from mScarlet-I and Neongreen proteins lags mRNA expression as the proteins must be translated and then folded into the mature fluorescent state. Together, these data indicate that, as expected, euo mRNA is expressed in RBs (double positive for euoprom signal and euo mRNA signal), while hctA mRNA is expressed in IBs (hctAprom+, hctA mRNA+ and hctBprom negative) and hctB mRNA is

281 expressed in late IB/EBs (hctBprom+ and hctB mRNA+). Therefore, we used this workflow to interrogate cell
282 form gene expression predicted by the RNA-seq clustering, binning and volcano plot analysis.
283
284 **Validation of *porB* as an IB gene.** We next sought to determine if a gene predicted to be expressed in a
285 particular cell form by the RNA-seq clustering experiment could be verified. The porin gene *porB* [29] which
286 clustered with the IB gene group (Fig. 2B) as well as with hctA (a proven IB gene) was selected for the
287 analysis. Cells were infected with either L2-AsciEng or L2-BsciEng, fixed at 24 hpi and probed for the *porB*
288 mRNA. Confocal images were taken and viewed as z projections (Fig. 5A). The *porB* mRNA signal (magenta)
289 did not completely overlap with the euoprom signal (green) and appeared to be expressed in a subset of cells
290 (Fig. 5A). The *porB* mRNA had significant but not complete overlap with the *hctA*prom+ cells (green) and
291 almost no overlap with the *hctB*prom+ cells (Fig. 5A). Using the TrackMate protocol described above we
292 identified the promoter reporter expressing populations, *euo*prom, *hctA*prom, and *hctB*prom (green) and then
293 separately, the *porB* mRNA+ population (magenta) and measured the fluorescence intensity of each channel
294 (fluorescent reporter proteins and mRNA signal within each population). The *porB* mRNA+ population
295 (magenta) in the *euo*prom channel experiment were a mix of single and double positive cells. This was also
296 true for the euoprom+ population (green). In comparison, the *porB* mRNA+ population (magenta) in the
297 *hctA*prom channel experiment were primarily double positive, i.e. high *porB* mRNA and high *hctA*prom activity.
298 However, the *hctA*prom+ population (green) was a mix of single positive and double positive cells (Fig. 5A). In
299 the *hctB*prom channel experiment, the *porB* mRNA signal+ population (magenta) were primarily single positive
300 and did not have appreciable *hctB*prom fluorescence. Conversely the *hctB*prom+ population (green) was
301 primarily single positive with low *porB* mRNA signal. Taken together, the *porB* mRNA expression pattern was
302 similar to that of the *hctA* mRNA expression pattern strongly suggesting *porB* is expressed primarily in the IB
303 cell form.
304 We also evaluated the kinetics of the activity of the *porB* promoter. The *hctA* promoter from AsciEng
305 was replaced with the promoter region of *porB* (-137bp to +30bp) and transformed into *Ctr* to create L2-
306 PsciEng. We used live cell imaging to measure the expression of Neongreen driven by *euo*prom and mScarlet-
307 I driven by *porB*prom. Cells were infected with PsciEng at an MOI ~0.3 and imaged for both the Neongreen
308 and mScarlet-I fluorescence every 30 minutes from 10 hpi for 55 hours. For comparisons, L2-AsciEng and L2-
309 BsciEng strains were imaged in parallel. As previously published, *euo* promoter activity is detected at ~12 hpi
310 followed by the *hctA* promoter and finally the *hctB* promoter [8,9] (Fig. 5B). The kinetics of L2-PsciEng mirrored
311 that of L2-AsciEng. *Euo*prom activity was detected at ~12 hpi followed by the activity of the *porB*prom at ~20
312 hpi followed by *hctB*prom activity starting at ~26 hpi. Taken together these data suggest that *porB*, as
313 predicted by the RNA-seq clustering experiment, can be considered an IB gene.
314
315 **Predicted cell type expression of T3SS genes.** We noticed an intriguing expression pattern with the type III
316 secretion system (T3SS) structural genes in the clustering data that suggested cell form specific expression.
317 To explore this observation, we plotted the effects of ectopic expression on the T3SS operons. We used our wt
318 RNA-seq data [30], operon prediction software [31] and the RT-PCR data published by Hefty et. [32] to annotate the
319 T3SS operons (Table S2) and plotted the expression data using volcano plots. These plots showed that the
320 majority of the T3SS operons were regulated in an IB like pattern, i.e. up-regulated between 18 hpi and 24 hpi,
321 repressed by Euo and HctB ectopic expression, but not induced by CtcB or HctA ectopic expression (Fig. 6).
322 The exception to this pattern were the two operons for the T3SS translocons, (*CTL0238, lcrH, copB_2,*
323 *copD_2*) and (*scc2, CTL0840, copB, copD*). The *CTL0238* operon (*CTL0238*-op) was regulated like an RB
324 gene while the *scc2* operon (*scc2*-op) was regulated like an EB gene (Fig. 6).
325
326 **Cell type expression of T3SS genes by FISH.** We next investigated the cell type expression of two of the
327 T3SS operons predicted to be expressed in the IB, the *sctU* operon and the *sctL* operon. The *sctU* operon

328 (*sctU*-op) encodes the genes *sctU*, *sctV*, *lcrD*, *copN*, *scc1*, and *malQ*, while the *sctL* operon (*sctL*-op) includes
329 the genes *sctL*, *sctR*, *sctS*, and *sctT* We used custom FISH probes encompassing *sctU* through *lcrD* for the
330 detection of the *sctU-op* mRNA and *sctL* to *sctR* for the detection of *sctL*-op mRNA. Cell monolayers were
331 infected with L2-AsciEng and L2-BsciEng at an moi ~ 0.3 and processed for FISH staining at 16 and 24 hpi
332 (Fig. 7 and Fig. S2). FISH signal was not observed in the RB cells (*euo*prom+) at 16 hpi for either *sctU*-op (Fig.
333 7A) or *sctL*-op (Fig. S2A). In the infections fixed at 24 hpi, the FISH staining for both operons was observed in
334 cells distinct from *euo*prom+ and *hct*Bprom+ cells (Fig. 7B and Fig. S2B). However, both T3SS operon mRNAs
335 were detected in a subset of the *hctA*prom+ cell population (Fig. 7B and Fig. S2B). We next used our
336 TrackMate workflow to quantitate these data. Cells were identified by their promoter reporter signal (green) and
337 separately by their mRNA fluorescence signal (magenta). The fluorescence intensity was measured and
338 plotted for both channels (FISH (magenta) and promoter reporter (green)) in both identified populations as
339 described in Fig. 4.
340 **Expression in RB cells.** We identified the mRNA+ cell population (magenta) and quantified both the
341 *euo*prom signal intensity and the FISH signal intensity. For both the *sctU*-op and the *sctL*-op there was
342 primarily a double positive population (high mRNA signal and high *euo*prom signal). We also quantified the
343 mRNA expression in RBs by identifying the *euo*prom+ cells (green) and measuring the *sctU*-op (Fig. 7C) and
344 sctL-op (Fig. S2C) FISH signal and plotted this against the *euo*prom signal intensity. The *euo*prom+ population
345 (green) were both single and double positive for both operons (Fig. 7C and Fig. S2C, *euo*p). These data
346 suggest that neither operon was expressed in RBs. As there was no mRNA signal in the 16 hpi RB cells, it is
347 likely that the mRNA+ double positive cell population at 24 hpi were IBs with carryover Neongreen signal, while
348 the *euo*prom+ single positive population were the RBs.
349 **Expression in IB cells.** The mRNA+ cell population (magenta) was identified and both the *hctA*prom
350 signal intensity and the FISH signal intensity was quantified and plotted. For both the s*ctU*-op (Fig. 7C) and
351 *sctL*-op (Fig. S2C) mRNA+ cells (magenta), the majority were double positive for mRNA signal and *hctA*prom
352 signal. For the *hctA*prom+ cell population (green) there was both a single (*hctA*prom) and double positive
353 (*hctA*prom and mRNA) population (Fig. 7C and Fig. S2C, *hctA*p). These data further suggest that the *sctU*-op
354 and *sctL*-op were expressed in the IB cell type. It's likely that the *hctA*prom+ single positive population are late
355 IB/EB cell forms that are becoming EBs and have repressed *sctU*-op and *sctL*-op expression.
356 **Expression in EB cells.** In contrast, the mRNA+ cell population for both the *sctU*-op and the *sctL*-op in
357 the hctBprom expressing cells were distinct single positive (mRNA signal) populations (Fig. 7C and Fig. S2C,
358 *hctB*p). Additionally, the *hctB*prom+ cell population was also primarily single positive (*hctB*prom). These data
359 suggest that the sctU-op and the sctL-op were not expressed in the EB cell forms. Combined, these overall
360 expression patterns of the *sctU* and *sctL* operons were very similar to that of the *hctA* mRNA and *porB* mRNA
361 FISH, supporting an IB like gene expression pattern.
362
363 **Cell type expression of the T3SS translocon genes by FISH.** As mentioned above, the *Ctr* genome
364 encodes two operons for the T3SS translocon each of which contain four genes, the *CTL0238*-op and the
365 *scc2*-op [33]. This duplication is conserved in all the vertebrate infecting chlamydial species. The expression
366 profiles from our clustering data and volcano plots suggested that the two translocon operons are expressed in
367 different cell types; the *CTL0238*-op in RBs and the *scc2*-op in EBs (Fig. 6). To verify differential cell type
368 expression, host cells were infected with L2-BsciEng, fixed at 24 hpi and probed with custom FISH probes
369 designed against C*TL0238*-op and *scc2*-op. These infected and FISH stained cells were imaged by confocal
370 microscopy. The confocal micrographs showed that the mRNA FISH signal for *CTL0238*-op heavily overlapped
371 with the *euo*prom channel but was distinct from *hctB*prom+ cells (Fig. 8A, *CTL0238*-op mRNA). In contrast, the
372 mRNA signal for the *scc2*-op was distinct from the *euo*prom+ cells but almost completely overlapped the
373 *hctB*prom+ cells (Fig. 8B, *scc2*-op mRNA).

We again quantified this expression pattern using our TrackMate workflow. Chlamydial cells were identified by their promoter reporter signal (green) and separately by their mRNA fluorescence signal (magenta). The fluorescence intensity was measured and plotted for both channels, FISH (magenta) and promoter reporter (green).

Expression in RB cells. We identified the CTL0238-op mRNA+ cell population (magenta) and quantified both the euoprom signal intensity and the FISH signal intensity. For the CTL0238-op mRNA+ cells, there was primarily a double positive population (high mRNA signal and high euoprom signal) (Fig. 8A). We also quantified the mRNA expression in RB cells (*euo*prom+ cells, green) The CTL0238-op FISH signal was plotted against the *euo*prom signal intensity and the euoprom+ cells (green) were mostly double positive with an additional single positive population (Fig. 8A). This single positive (euoprom+, CTL0238-op mRNA-) population is likely due to the long half life of the GFP protein.

Expression in EB cells. In contrast, the CTL0238-op mRNA+ cell population (megenta) when plotted for mRNA signal and the hctBprom signal was a distinct single positive population (CTL0238-op mRNA+, hctBprom-) (Fig. 8A). We also identified the hctBprom+ cell population (green) and plotted the mRNA signal and hctBprom signal. This population was also primarily single positive (hctBprom+, CTL0238-op mRNA-).

For the scc2-op mRNA FISH quantification the results were opposite. The scc2-op+ cells (megenta) were primarily single positive when plotted against the euoprom signal and double positive when plotted against the hctBprom signal (Fig. 8B). While the euoprom+ cell population (green) was also primarily single positive and the hctBprom+ cells (green) were primarily double positive (Fig. 8B).

To further highlight the differential expression of *CTL0238*-op mRNA and *scc2*-op mRNA, we infected cells with L2 AsciEng and processed the samples for FISH at 16 hpi when most of the chlamydial cells are RBs. At 16 hpi essentially all the cells were green RBs (*euo*prom+) with little to no red IBs (*hctA*prom+) cells. The green *euo*prom+ cells were all positive for the *CTL0238*-op FISH signal (Fig. 8C, *CTL0238*-op). In contrast, the *scc2*-op FISH signal was undetectable in *euo*prom+ cells (Fig. 8D, *scc2*-op). Taken together, these data support the observation that the two translocon operons are differentially regulated and are expressed in distinct cell forms. The *scc2*-op is expressed in late IB/EB cells while the *CTL0238*-op is expressed in RB cells.

Predicted cell type expression of T3SS effectors. In general, T3SS translocons are involved in interacting with host membranes to facilitate the secretion of T3SS effectors into target cells [34]. During infection, *Ctr* secretes effectors into/through two membrane systems, the host cell plasma membrane and, once inside the cell, the inclusion membrane. Additionally, the chlamydial T3SS is known to secrete different kinds of effectors, soluble proteins as well as the integral membrane inclusion (Inc) proteins [35–38]. Using volcano plots we asked how the genes encoding the soluble effector proteins (Table S3) and Inc proteins (Table S4) were regulated by the ectopic expression of Euo, HctA, HctB and CtcB. The vast majority of the soluble T3SS effector genes were regulated like EB genes; higher in 18-24 hpi and induced by HctA and CtcB ectopic expression, but down regulated by Euo and HctB ectopic expression (Fig. 9A). In contrast, most of the *incs* were regulated like RB genes with the exception of *incM* and *incV,* which were regulated like EB genes (Table S4 and Fig. 9B).

Cell type expression of *inc* genes by FISH. The volcano plots suggested that the majority of the *inc* effector genes were expressed in an RB like pattern. However, two Inc genes (*incV* and *incM)* stood out as potential EB genes (Fig. 9B). To determine if the putative late Inc, *incV,* was expressed late in RBs or was a bona fide EB gene, we compared mRNA expression of a known RB expressed Inc, *incD* to *incV* using FISH. Cells infected with L2-BsciEng were probed for the expression of *incD* and *incV* at 16 hpi (mostly RBs) and 24 hpi (all three cell forms). Confocal microscopy revealed that, as expected, *incD* was expressed in *euo*prom+ RB cells at both 16 hpi and 24 hpi and not in *hctB*prom+ EBs present at 24 hpi (Fig. 10A). Conversely, *incV* mRNA could not be detected at 16 hpi and was expressed exclusively in *hctB*prom+ EBs (Fig. 10B).

Again, we quantified expression of each gene in RBs and EBs from inclusions from the 24 hpi experiments using our TrackMate workflow. Chlamydial cells were identified by their promoter reporter signal (green) and separately by their mRNA fluorescence signal (magenta) and the signal for both populations was plotted.

Expression in RB cells. We identified the incD mRNA+ cell population (magenta) and plotted both the euoprom signal intensity and the FISH signal intensity (Fig. 10C). For the incD mRNA+ cells there was primarily a double positive population (high incD mRNA signal and high euoprom signal). We also quantified the mRNA expression in RB cells (*euo*prom+ cells, green) The incD FISH signal was plotted against the euoprom signal intensity and the euoprom+ cells (green) were mostly double positive with an additional small single positive population. This single positive (*euo*prom+, incD mRNA-) population is likely due to the long half life of the GFP protein allowing it to also label early IB cells forms.

Expression in EB cells. In contrast, the incD mRNA+ cell population (magenta) when plotted for mRNA signal and the hctBprom signal was a distinct single positive population (incD mRNA+, hctBprom-) (Fig. 10C). We also identified the hctBprom+ cell population (green) and plotted the mRNA signal and hctBprom signal. This population was also primarily single positive (hctBprom+, incD mRNA-).

For the incV FISH signal the results were opposite. The incV+ cells (magenta) were primarily single positive when plotted against the euoprom signal and double positive when plotted against the hctBprom signal (Fig. 10D). While the euoprom+ cell population (green) was also primarily single positive and the hctBprom+ cells (green) were primarily double positive (Fig. 10D). These data support the hypothesis that incD is indeed an RB gene and that incV, and likely incM, are EB genes.

Discussion:

The chlamydial developmental cycle has traditionally been defined by the timeline of the infection. The infectious EB invades the host cell and begins EB to RB differentiation into the RB cell form that then begins to divide. The genes involved in this process have been described as the early genes. Sometime after EB to RB differentiation and the initiation of replication transitionary forms appear. The gene expression associated with this timeframe is usually considered the chlamydial midcycle. At ~24 hpi until cell lysis EBs accumulate in the inclusion. Genes upregulated at this time point and forward are considered late genes [14–16]. We have dissected the developmental cycle and developed a model based on cell type transitions [9]. Our model suggests that the developmental cycle is best described by a programmed cell production model [9]. In this model, the EB enters the host cell (through the use of premade effectors) and initiates immediate early protein synthesis (EB to RB differentiation genes) to begin the EB to RB differentiation process. The EB to RB differentiation process takes ~ 10 hours to complete. The completion of EB to RB differentiation is defined by the first division of the nascent cell resulting in RB cells. At this stage the RBs expand in number through cell division, amplifying the infection. Our model suggests the RBs mature during this amplification stage, ultimately producing daughter cells with asymmetric fates. One daughter cell becomes the IB cell form while the other remains an RB. Our model defines the IB cell form as the committed cell to EB formation. The mature RBs at this stage continue to replicate producing one IB and one RB. The IBs never re-enter the cell cycle and instead transition into the infectious EB form which takes ~ 10 hours to complete [9].

In this study, we ectopically expressed four transcriptional regulatory proteins that all blocked the progression of the developmental cycle. The effects of expression of these regulatory proteins using RNA-seq was determined and compared using a clustering algorithm which resulted in three distinct regulation patterns. The first cluster contained genes that were unaffected by the ectopic expression of Euo and were not upregulated between 18 hpi and 24 hpi of a *Ctr* L2 infection. The second cluster consisted of genes whose expression increased from 18 hpi to 24 hpi of a wt infection and were not induced by ectopic expression of HctA and CtcB. The third cluster of genes were upregulated between 18 hpi and 24 hpi and by the ectopic expression of both HctA and CtcB. These groups fit well into the major cell categories in our model; RBs, IBs and EBs. Using the clustering observation, we created selection criteria based on changes in gene expression

469 from our RNA-seq experiments. We were able to bin 639 out of 902 genes (~70%) into one of the RB, EB, and
470 IB categories. The genes that could not be assigned were either expressed at levels too low to have
471 confidence in the expression pattern, or had a unique expression pattern that did not fit into the three
472 categories suggesting potential unique roles in chlamydial biology. This study focused on determining gene
473 expression through measuring mRNA and it remains to be determined if any of these genes are translationally
474 regulated as well.

475 The RB cell is the replicating cell form leading to expansion of cell numbers. Based on the changes in
476 gene expression after ectopic expression of Euo, HctA, CtcB and HctB we found that 532 genes were
477 regulated as RB genes. This category included cell replication genes, genes involved in protein synthesis,
478 genes for many of the Inc proteins and the *euo* gene. Based on our selection criteria this group likely
479 encompasses both potential constitutive genes (expressed in RBs, IBs and potentially early EBs) as well as
480 RB specific genes such as *euo*, *incD* and the *CTL0238*-op which were expressed only in the RB cell form.

481 The IB cell type is the transitional form between the RB and the EB and is currently poorly defined. We
482 define the IB cell type as the committed step to EB formation; the IB is the cell form that exits the cell cycle and
483 begins the program to transition into the infectious EB [9]. Our data identified 67 genes that are likely expressed
484 specifically in the IB cell type. The functions of these genes vary widely. We identified two porin genes (*porB*
485 and *CLT0626*), two disulfide isomerases (*CTL0149* and *CTL0152*) and six polymorphic outer membrane
486 proteins (*pmpB*, *C, E*, *F*, *G*, and *H*) as IB genes suggesting dramatic changes to the outer membrane of the IB
487 as it transitions into the EB.

488 The EB cell is the infectious cell form that is "terminally" differentiated. Once formed in the inclusion, the
489 EB maintains an infectious phenotype through active metabolism but has very low levels of protein expression
490 as shown by click chemistry and the EBs ability to maintain infectivity in the presence of protein synthesis
491 inhibitors while inside the inclusion, and by the requirement of nutrients for the EB to maintain infectivity in the
492 presence of protein synthesis inhibitors after cell exit [30]. Here, we define the EB regulon as the genes
493 expressed during the late IB to EB maturation phase resulting in the infectious form. Of the 46 EB genes, 18
494 had been previously shown to be directly regulated by the sigma54 alternative sigma factor and 4 were
495 reported to be sigma28 regulated genes [24,27]. The regulation of the remaining 24 genes is unknown. As both
496 HctA ectopic expression and the ectopic expression of CtcB induce the expression of the EB genes, the EB
497 regulon is likely regulated by a complex shift in gene expression and activation of the sigma54 and sigma28
498 regulons is a part of this shift.

499 We tested one of the predicted IB genes, *porB*, and showed that its regulation, both by promoter
500 specific gene expression in chlamydial cells and by its developmental kinetics, matched that of *hctA.* This was
501 further confirmed using FISH to demonstrate cell type gene expression matched that of the IB gene, *hctA*. We
502 have previously published the kinetics of the *euo*, *hctA* and *hctB* promoters and showed that the promoter
503 activities fit into the RB, IB and EB model [8,9]. Here we combined these promoter reporter strains with FISH and
504 demonstrated that the *euo* mRNA was expressed primarily in RBs, that *hctA* mRNA was expressed in IBs, and
505 that *hctB* mRNA was expressed in EBs demonstrating the usefulness of FISH for identifying cell type specific
506 gene expression.

507 Overall, these data support a model that includes (at least) three dominant cell forms: the RB, the IB
508 and the EB. These cells have dramatically different gene expression profiles and phenotypes. The EB has
509 been well characterized as it is the infectious form, does not replicate and has a dramatically condensed
510 nucleoid. The nucleoid structure is due in part to the binding of the two histone like proteins, HctA and HctB to
511 the chromosome [19,22]. Our data indicates that the construction of the compact nucleoid occurs in two distinct
512 and temporally separated steps [8,9]. HctA is expressed as an IB gene and, when ectopically expressed, resulted
513 in the expression of the EB genes suggesting that HctA expression is an important regulator of the IB to EB
514 transition. HctB on the other hand is expressed as an EB gene and, when ectopically expressed, resulted in
515 the inhibition of the expression of most genes with the exception of the ribosomal protein genes. An intriguing

516 hypothesis is that the ribosomal protein genes are potentially free of inhibition and that protein synthesis could
517 be rapidly reinitiated upon EB to RB differentiation, before complete removal of HctA and HctB from the
518 chromosome. Taken together, these data suggest that the transition from the IB to EB occurs in two steps; 1)
519 HctA chromosomal binding turns off RB and IB genes, allowing EB genes to become expressed, and 2) HctB
520 is expressed late in EB formation creating the final condensed nucleoid that potentially spares the ribosomal
521 genes.

522 Volcano plots of the effects of ectopic expression of the four regulatory genes support the
523 categorization of most chlamydial genes into the RB, IB and EB categories. We specifically focused on the
524 expression of the T3SS operons and observed that the majority of the operons for the structural components
525 were IB-like in their regulation. This was verified using FISH for both the *sctL* operon (*sctL, sctR, sctS, and*
526 *sctT*) and the *sctU* operon (*sctU, sctV, lcrD, copN, scc1, and malQ*). While the majority of the T3SS structural
527 operons were expressed as IB genes, the two translocon operons (*CTL0238, lcrH, copB_2, copD_2*) and
528 (s*cc2, CTL0840, copB, copD*) were predicted by clustering and volcano plots to be expressed in RB and EB
529 cells respectively. This prediction was again verified by FISH in the context of dual promoter reporter strains.

530 The observation that the two translocons were expressed in distinct cell forms (*CTL0238*-op in RBs and
531 *scc2*-op in EBs) prompted us to determine the expression of the T3SS effectors. *Ctr* encodes two classes of
532 effectors, soluble and inclusion membrane embedded proteins (Incs) [36,39,40]. The data from this study showed
533 that the majority of the Inc protein effectors (28 out of 36) were expressed as RB genes while the majority of
534 the soluble T3SS effectors (17 out of 23) were expressed as EB genes and that none of the soluble effectors
535 were expressed as RB genes. This pattern suggests an intriguing hypothesis; the *scc2*-op translocon
536 translocates soluble effectors as the EB contacts host cells and mediates entry events, while the *CTL0238*-op
537 is expressed early during the EB to RB differentiation process in the nascent inclusion and translocates the
538 transmembrane Inc effectors. Whether this separation is temporal or whether the two translocons are
539 specialized for the translocation of soluble vs. inclusion membrane effectors is currently unknown. Interestingly,
540 although the majority of the Inc proteins were expressed as RB genes there were two Incs that were
541 determined to be expressed in EBs, *incV* and *incM*. In addition to its regulation pattern, we also verified that
542 *incV* was an EB gene using FISH. Both IncV and IncM are involved in the establishment of early inclusion
543 functions [41,42]. We hypothesize that these "pre-loaded" Inc proteins are among the first to be secreted from
544 internalized *Ctr* after the *CTL0238*-op is deployed.

545 *Ctr* communicates and reprograms the host cell to create and maintain its intracellular replication niche
546 in part through the use of the T3SS. We were surprised that the majority of the T3SS operons for the structural
547 components of the system were expressed as IB genes. This expression pattern along with the cell type
548 specific expression of the translocons (one in the RB and one in the EB) and effectors suggests that the T3SS
549 is constructed, deployed and secretes effectors in a cell type specific manner that is likely a critical component
550 of the complex developmental cycle and host cell reprogramming.

551 Taken together, these data support our overall model that the chlamydial developmental cycle should
552 be viewed as consisting of discrete phenotypic cell forms that are produced by an underlying developmental
553 program consisting of RBs that amplify the infection, RBs that produce IBs and IBs that transition into the
554 infectious EB [8,9] (Fig. 11). This process creates an infection with mixed phenotypic forms throughout the
555 infection. The data also suggest that each cell type has a distinct gene expression profile (RB, IB and EB) and
556 that the relative numbers of each of these cell forms creates the time based expression patterns reported in
557 population based studies [13–16]. Our model suggests that the EB binds to and enters cells in part through the
558 deployment of soluble effectors and the *scc2*-op translocon expressed during EB development. After entry, EB
559 to RB differentiation begins and the RB genes are expressed including the *CTL0238*-op translocon which
560 deploys the Inc proteins for the creation of the inclusion replication niche and the genes required for chlamydial
561 replication leading to RB amplification. After an amplification period, the RB matures into a stem cell-like cell
562 form and begins to produce IBs [9]. The IB synthesizes the T3SS structural components and matures into the

563 EB form over ~8-10 hours. That the IB and not the RB expresses the genes for the construction of the T3SS
564 suggests that the T3SS apparatus that entered on the EB cells remains on the RBs and is diluted with every
565 replication. It is unclear if the secretion system gets partitioned equally or is retained in a subset of RBs.
566 Intriguingly, this supports a proposed role of T3SS dilution in cell form maturation/development put forth
567 previously [37,43,44].
568 The IB also expresses the histone like DNA binding protein, HctA. Previous studies have shown that
569 when expressed in *E. coli*, HctA can alter gene expression in a gene specific manner [19]. Our data suggest that
570 HctA has an important role in shifting gene expression from the IB pattern to the EB genes. This is likely in
571 conjunction with the CtcB/C two component regulatory system and the sigma54 alternative sigma factor [24,27].
572 The EB genes as previously mentioned include the majority of the soluble T3SS effectors and the *scc2*-op
573 translocon as well as the HctB DNA binding protein. We hypothesize that EB gene expression loads the EB
574 with the invasion-related proteins and HctB shuts down the majority of gene expression creating the dense
575 nucleoid, the final step of EB formation. This prepares the EB for the initiation of the next round of infection
576 (Fig. 11). Our data has highlighted three categories of gene expression that define the three major phenotypic
577 cell forms, RB, IB and EB. However, future studies are needed to define the regulatory circuits and DNA
578 elements that create these cell form expression patterns.
579 DNA replication is tightly controlled during the *Ctr* developmental cycle; only the RB cell form replicates
580 the chromosome and the IB and EB cells contain a single fully replicated chromosome [45]. The role of the
581 control of DNA replication in regulating gene expression is currently unknown. However, it is intriguing to
582 speculate that DNA replication could contribute to changes in DNA supercoiling which has been shown to play
583 a role in gene expression during the chlamydial developmental cycle [46–48]. Our identification of cell type gene
584 expression of a large percentage of the chlamydial genome will aid the determination of the functions of the
585 many hypothetical genes encoded in the chlamydial genome. Understanding the function of many of these
586 genes has been hampered by the mixed cell environment of the chlamydial inclusion. Additionally, with the
587 emerging genetic tools available to investigate the functional roles of genes during infection, knowing in which
588 cell type they are expressed will improve the interpretation of the results.
589
590 **Materials and Methods**
591
592 **Cell Culture**
593 Cell lines were obtained from the American Type Culture Collection. Cos-7 cells (CRL-1651) were grown in
594 RPMI-1640, supplemented with 10% FBS and 10 µg/mL gentamicin (Cellgro). *Chlamydia trachomatis* serovar
595 L2 (LGV Bu434) was grown in Cos-7 cells. Elementary Bodies (EBs) were purified by density gradient (DG)
596 centrifugation essentially as described [49] following 48 h of infection. EBs were stored at -80ºC in Sucrose
597 Phosphate Glutamate (SPG) buffer (10 mM sodium phosphate [8mM K2HPO4, 2mM KH2PO4], 220 mM
598 sucrose, 0.50 mM l-glutamic acid, pH 7.4) until use.
599
600 **Vector Construction**
601 All constructs used p2TK2-SW2 [50] as the backbone and cloning was performed using the In-fusion HD EcoDry
602 Cloning kit (FisherScientific). Primers and geneblocks (gBlocks) were ordered from Integrated DNA
603 Technologies (IDT) and are noted in Table S5. The construction and characterization of p2TK2-SW2-T5-E-
604 clover-3xFLAG (E-clover), p2TK2-SW2-Tet-J-E-clover-3xFLAG (Tet-JE-clover) and p2TK2-SW2-Tet-J-E-hctB-
605 3xFLAG (Tet-JE-hctB) has been described previously [25].
606 <u>E-hctA-3xFLAG (E-hctA), E-euo-3xFLAG, (E-euo) and E-ctcB-3xFLAG (E-ctcB)</u>,
607 The *hctA*, *euo* and *ctcB* ORFs were amplified from *Ctr* L2(434) using the primers indicated in Table S5.
608 Each fragment was used to replace Clover in p2TK2-SW2-T5-E-clover-3xFLAG.

609 *hctB*prom Scarlet-*euo*prom neongreen (BsciEng), *hctA*prom Scarlet-*euo*prom neongreen (AsciEng) and
610 *porB*prom_Scarlet-*euo*prom_neongreen (PsciEng).
611 The gBlock mScartlet-I (Table S5) was cloned into BMELVA [9] to replace mKate which created the
612 construct BscieLVA. The degradation tag LVA was then removed from neongreen using the primers indicated
613 to create BsciEng. The *hcA* and *porB* promoters were amplified and used to replace the *hctB* promoter using
614 the primers indicated to create AsciEng and PsciEng respectively.
615
616 **Chlamydial Transformation and Isolation.**
617 Transformation of Ctr L2 was performed essentially as previously described [8]. Briefly, $1x10^8$ EBs + >2µg
618 DNA/well were used to infect a 6 well plate. Transformants were selected over successive passages with
619 1U/ml penicillin G or 500µg/ml spectinomycin as appropriate for each plasmid. The new strain was clonally
620 isolated via successive rounds of inclusion isolation (MOI, <1) using a micromanipulator. Clonality of each
621 strain was confirmed by isolating the plasmid, transforming into *E. coli* and sequencing six transformants.
622
623 **Replating Assay.**
624 *Ctr* were isolated by scraping the infected monolayer into media and pelleting at 17200 rcfs. The EB pellets
625 were resuspended in RPMI via sonication and seeded onto fresh monolayers in a 96-well microplate in a 2-fold
626 dilution series. Infected plates were incubated for 24 hours prior to fixation with methanol and stained with 4′,6-
627 diamidino-2-phenylindole (DAPI) and *Ctr* MOMP Polyclonal Antibody, FITC (Fishersci). The DAPI stain was
628 used for automated microscope focus and visualization of host-cell nuclei, and the anti-*Ctr* antibody was used
629 to visualize the *Ctr* to identify and count inclusions. Inclusions were imaged using a Nikon Eclipse TE300
630 inverted microscope utilizing a scopeLED lamp at 470nm and 390nm, and BrightLine band pass emissions
631 filters at 514/30nm and 434/17nm. Image acquisition was performed using an Andor Zyla sCMOS in
632 conjunction with µManager software. Images were analyzed using ImageJ software and custom scripts.
633 Statistical comparisons between treatments were performed using an ANOVA test followed by Tukey's Honest
634 Significant Difference test.
635
636 **Transmission Electron Microscopy**
637 For analysis of the structure of *Ctr* upon ectopic protein expression, cell monolayers were infected with the
638 indicated strain at an moi of 0.5 and induced with 0.5mM Theophylline at 15 hpi. Infected cells were released
639 from the plate with Trypsin-EDTA at 30 hpi, rinsed with 1xPBS and the pellet was fixed with EM fixative
640 (2%PFA, 2% Glutaraldehyde, 0.1M Phosphate Buffer, pH 7.2) overnight at 4ºC. Fixed pellets were rinsed and
641 dehydrated before embedding with Spurr's resin and cross sectioned with an ultramicrotome (Riechert Ultracut
642 R; Leica). Ultra-thin sections were placed on formvar coated slot grids and stained with uranyl acetate and
643 Reynolds lead citrate. TEM imaging was conducted with a Tecnai G2 transmission electron microscope (FEI
644 Company; Hillsboro, OR).
645
646 **RNA-Seq**
647 Expression of each of the ectopic proteins was induced at 15 hpi with either 0.5 mM theophylline and 30ng/ml
648 anhydrotetracycline (HctB) or 0.5 mM theophylline (Clover, HctA, CtcB and Euo). Total RNA was isolated from
649 the infected cells for each treatment from triplicate experiments. Briefly, the infected monolayer was scraped
650 into ice cold PBS, lysed using a Dounce homogenizer and the *Ctr* enriched over a 30% MD-76R pad. Total
651 RNA was isolated using TRIzol reagent (Life Technologies) following the protocol provided, and genomic DNA
652 was removed (TURBO DNA-free Kit, Invitrogen). Both prokaryotic and eukaryotic rRNAs were depleted using
653 Illumina Ribo-Zero Plus. The enriched RNA samples were quantified and the libraries built and barcoded by
654 the IBEST Genomics Resources Core at the University of Idaho. The libraries were sequenced by University of
655 Oregon sequencing core using the Illumina NovaSeq platform. The chlamydial specific reads were analyzed by

656 aligning to the published *Ctr* L2 Bu 434 genome using the Bowtie2 aligner software [51]. The aligned chlamydial
657 reads were quantified for each chlamydial ORF using HT-seq. Statistical analysis and normalization of read
658 counts was accomplished using DESeq2 in R [52]. Log2fold change and statistics were also calculated using
659 DESeq2. Heatmaps and hierarchical clustering were generated and visualized using Python with Pandas and
660 the Seaborn visualization package [26]. The raw reads and HT-seq counts are accessible from the NCBI's Gene
661 Expression Omnibus with the accession number of GSE262652 and GSE276506. Volcano plots were
662 constructed from the log2fold change data using Python and the Bokeh plotting library (Bokeh Development
663 Team).
664
665 Total RNA was isolated from cells infected with the indicated strains. Expression of each protein was induced
666 at 15 hpi with either 0.5 mM theophylline and 30ng/ml anhydrotetracycline (HctB) or 0.5 mM theophylline
667 (Clover, HctA, CtcB and Euo) and the *Ctr* isolated at 18 and 24 hpi on ice. Briefly, the infected monolayer was
668 scraped into ice cold PBS, lysed using a Dounce homogenizer and the *Ctr* isolated over a 30% MD-76R pad.
669 Total RNA was isolated using TRIzol reagent (Life Technologies) following the protocol provided and genomic
670 DNA removed (TURBO DNA-free Kit, Invitrogen). The enriched RNA samples were quantified and the libraries
671 built and barcoded by the IBEST Genomics Resources Core at the University of Idaho. The libraries were
672 sequenced by University of Oregon sequencing core using the Illumina NovaSeq platform. RNA-seq reads
673 were aligned to the published *Ctr* L2 Bu 434 genome using the Bowtie2 aligner software [51]. Reads were
674 quantified using HTseq . Statistical analysis and normalization of read counts was accomplished using
675 DESeq2 in R [52]. Log2fold change and statistics were also calculated using DESeq2. Heatmaps and
676 hierarchical clustering were generated and visualized using Python with Pandas and the Seaborn visualization
677 package [30]. Aligned reads are accessible from the NCBI's Gene Expression Omnibus with the accession
678 number of GSE262652. Volcano plots were constructed from the log2fold change data using Python and the
679 Bokeh plotting library (Bokeh Development Team).
680
681 **RNA fluorescence in situ hybridization (RNA-FISH)**
682 All FISH probes were designed by Molecular Instruments (Los Angeles, CA) using the sequence indicated in
683 (Tabel S6). Cos7 monolayers seeded on coverslips were infected with the indicated strains at an MOI ~ 0.3.
684 Infected cells were fixed at the indicated times in 4% paraformaldehyde (PFA) for 10 min at RT at 24 hpi,
685 washed 2x with 1XPBS and dehydrated overnight at -20ºC in 70% EtOH. Samples were probed and the signal
686 was amplified as described by the protocol provided by Molecular Instruments with the exception that DAPI
687 was added to the final wash to visualize DNA. Coverslips were mounted on a microscope slide with MOWIOL®
688 mounting solution (100 mg/mL MOWIOL® 4-88, 25% glycerol, 0.1 M Tris pH 8.5).
689 Fluorescence images were acquired using a Nikon spinning disk confocal system with a 60x oil-
690 immersion objective, equipped with an Andor Ixon EMCCD camera, under the control of the Nikon elements
691 software. Images were processed using the image analysis software ImageJ (http://rsb.info.nih.gov/ij/).
692 Representative confocal micrographs displayed in the figures are maximal intensity projections of the 3D data
693 sets, unless otherwise noted.
694
695 **Live cell imaging**
696 Monolayers of Cos7 cells were grown in a glass bottom 24 well plate and infected with the promoter reporter
697 strains L2-BsciEng, L2-AsciEng and L2-PsciEng. Live cell imaging of the developing inclusions was started at
698 8 hpi using an automated Nikon epifluorescent microscope equipped with an Okolab (http://www.oko-
699 lab.com/live-cell-imaging) temperature controlled stage and an Andor Zyla sCMOS camera
700 (http://www.andor.com). Multiple fields of view from each well were imaged every fifteen minutes. The
701 fluorescence intensity of each inclusion over time was tracked using the ImageJ plugin TrackMate [28] and the
702 results were averaged and plotted using python and matplotlib [53].

703
704 **Figure 1.** Ectopic expression of Euo, HctA, CtcB and HctB resulted in inhibition of the developmental cycle. **(**A)
705 Cos-7 cells were infected with the four strains and a Clover control strain and induced for ectopic expression at
706 15 hpi. EBs were harvested at 48 hpi. IFU production was dramatically reduced by the ectopic expression of
707 Euo, HctA, CtcB and HctB but not by the expression of the Clover protein. * = P < 0.01. (B) Transmission EM
708 of Cos-7 cells infected with *Ctr* expressing Clover, Euo, HctB, HctA or CtcB. Ectopic expression was induced at
709 15 hpi and the cells were fixed and stained at 30 hpi. The bacteria in the Clover induced and uninduced
710 chlamydial infections looked similar with inclusions of both samples containing large RB like cells as well as
711 electron dense EB like cells. The *Ctr* in the Euo expressing inclusions were primarily RB like cells while very
712 few cells were electron dense EB cells. The chlamydial cells in the HctB expressing inclusions were abnormal
713 looking, some with apparent condensed nucleoids. The HctA expressing *Ctr* also appeared abnormal with
714 condensed nucleoids. Many of the CtcB expressing *Ctr* cells were target-like RB sized cells with a condensed
715 nucleoid.
716
717 **Figure 2.** RNA-seq analysis of *Ctr* ectopically expressing Euo, HctA, HctB, or CtcB. **(**A) For each of the
718 induced samples (n=3) the RNA-seq PCA profiles clustered within the same ectopic expression group but each
719 group had a distinct profile as visualized by plotting the first and second principal component. (B and C) The
720 cluster plots revealed two distinct late gene regulation groups. (B) The IB gene cluster was defined as those
721 that were upregulated between wt *Ctr* infections at 18 hpi and 24 hpi but were not upregulated by the ectopic
722 expression of HctA and CtcB as compared to the Clover control. (C) The EB gene cluster was defined as
723 genes that were upregulated between wt *Ctr* infections at 18 hpi and 24 hpi and were induced by ectopic
724 expression of HctA and CtcB as compared to the Clover control.
725
726 **Figure 3.** Effects of ectopic expression of Euo, HctA, CtcB and HctB on the gene expression of every *Ctr* gene.
727 RNA-seq differential expression was determined for each gene using DESeq2 for native infection at 18 hpi vs
728 24 hpi, Euo-FLAG expression, HctA-FLAG expression, CtcB-FLAG expression and HctB-FLAG expression vs
729 the control Clover-FLAG. Volcano plots show that the expression of RB designated genes (orange) were
730 largely unchanged from 18 hpi to 24 hpi while IB (green) and EB (red) designated genes were dramatically up
731 regulated. For Euo-FLAG expression the RB genes (orange) were largely unchanged while IB genes (green)
732 and EB genes (red) were all down regulated. Ectopic expression of HctA-FLAG resulted in the repression of
733 many of the RB genes (orange) and up regulation of the EB genes (red) but had little impact on the expression
734 of the IB genes (green). CtcB-FLAG expression had very little effect on RB genes (orange) but dramatically
735 upregulated EB genes (red). The ectopic expression of HctB-FLAG resulted in the down regulation of both IB
736 (green) and EB (red) genes but up-regulated many RB genes (orange). Additionally, HctB-FLAG expression
737 resulted in the upregulation of many of the ribosomal protein genes (purple).
738
739 **Figure 4.** Cell type expression of representative genes from the three gene categories (RB, IB and EB)
740 correspond to the three chlamydial cell forms. Cos-7 cells infected with L2-AsciEng or L2-BsciEng, fixed at 24
741 hpi and stained using FISH probes for *euo* mRNA, *hctA* mRNA and *hctB* mRNA. (A) Z-projection confocal
742 micrographs showing *euo* mRNA localization in comparison to *euo*prom, *hctA*prom and *hctB*prom activity.
743 Individual chlamydial cells with *euo* mRNA signal from 5 inclusions were identified using TrackMate and the
744 fluorescence intensity for each channel (mRNA and promoter reporter) was plotted (magenta dots). Individual
745 chlamydial cells positive for *euo*prom, *hctA*prom or *hctB*prom signal from 5 inclusions were also identified using
746 TrackMate and their expression intensity for each channel was plotted (green dots). (B) Z-projection confocal
747 micrographs showing *hctA* mRNA localization in comparison to *euo*prom, *hctA*prom and *hctB*prom activity.
748 Individual chlamydial cells with *hctA* mRNA signal from 5 inclusions were identified using TrackMate and the
749 fluorescence intensity for each channel (mRNA and promoter reporter) was plotted (magenta dots). Individual

750 chlamydial cells positive for *euo*prom, *hctA*prom or *hctB*prom signal from 5 inclusions were also identified using
751 TrackMate and their expression intensity for each channel was plotted (green dots). (C) Z-projection confocal
752 micrographs showing *hctB* mRNA localization in comparison to *euo*prom, *hctA*prom and *hctB*prom activity.
753 Individual chlamydial cells with *hctB* mRNA signal were identified from 5 inclusions using TrackMate and the
754 fluorescence intensity for each channel (mRNA and promoter reporter) was plotted (magenta dots). Individual
755 chlamydial cells positive for *euo*prom, *hctA*prom or *hctB*prom signal from 5 inclusions were also identified using
756 TrackMate and their expression intensity for each channel was plotted (green dots). Size bar = 5µm.
757
758 **Figure 5.** PorB gene expression is consistent with being classified as an IB gene. **(**A) FISH analysis of *porB*
759 mRNA expression in comparison to *euo*prom, *hctA*prom and *hctB*prom activity at 24 hpi. Confocal micrographs
760 of L2-AsciEng and L2-BsciEng infected cells probed for *porB* mRNA expression from 5 inclusions using
761 Molecular instruments FISH probes. TrackMate was used to identify the *porB* mRNA+ cell population and
762 measure the FISH fluorescent signal as well as the *euop*rom, *hctA*prom and *hctB*prom fluorescent signal. The
763 intensity for both channels for each cell was plotted (magenta dots). The *euo*prom, *hctA*prom and *hctB*prom+
764 cell population were also identified using TrackMate and the signal from the FISH channel and fluorescent
765 protein channels were plotted on the same graphs (green dots). (B) Cells were infected with L2-PsciEng and
766 the developmental gene expression kinetics were compared to those of L2-AsciEng, and L2-BsciEng. The
767 *euo*prom expression kinetics were comparable for all strains with expression first detected at ~15 hpi.
768 *PorB*prom expression kinetics were nearly identical to *hctA*prom expression kinetics, first detected at ~20 hpi,
769 while *hctB*prom expression was initiated at ~26 hpi. Error cloud for fluorescent reporters represents SEM.
770 n > 20 inclusions per strain.
771
772 **Figure 6.** The effects of ectopic expression of Euo, HctA, CtcB and HctB on T3SS structural genes. The
773 log2fold change RNA-seq differential expression data from the ectopic expression experiments were plotted
774 against the -log of the p value (-log padj) and the operons for the T3SS were highlighted. For the wt *Ctr* 18 hpi
775 vs 24 hpi samples most of the T3SS structural genes were upregulated while for the Euo ectopic expression
776 experiment most of these operons were downregulated. Again, like the IB genes in the HctA and CtcB ectopic
777 expression experiments, most of the structural genes were downregulated or unchanged. Two operons did not
778 follow this pattern, the *CTL0238*-op and *scc2*-op. Both operons encode the components of the T3SS
779 translocon. The *CTL0238*-op (gold circle) was regulaged like an RB gene while the *scc2*-op (purple circle) was
780 regulated like an EB gene.
781
782 **Figure 7.** IB cell type expression of the T3SS structural operon SctU. (A) Cells were infected with L2-AsciEng
783 for 16 hpi and fixed and stained using a FISH probe (*sctU-lcrD*) to the mRNA for the T3SS structural operon
784 sctU-op, the RB control *euo* and the IB control *hctA*. All cells were positive for *euo*prom expression (green).
785 The FISH stained cells were only positive for *euo* mRNA (magenta) and were negative for *hctA* mRNA
786 (magenta) and *sctU-op* mRNA (magenta). (B) Cells were infected with L2-AsciEng and L2-BsciEng for 24 hpi
787 and fixed and stained using FISH for the *sctU*-op mRNA. For the *euo*prom sample, the *sctU*-op FISH signal
788 (magenta) was present in a distinct subset of cells and not in the majority of the *euo*prom+ cells (green). (C)
789 TrackMate was used to identify the *sctU*-op mRNA+ cells from 5 inclusions from 24 hpi samples and the signal
790 for *euo*prom and FISH were quantified for each *sctU*-op+ cell and plotted (magenta dots). The converse was
791 also performed, the *euo*prom+ cells were identified and the *euo*prom signal and FISH signal was quantified for
792 each *euo*prom+ cell and plotted (green dots). The FISH signal was also compared to the *hctA*prom expression
793 pattern and showed subsets of cells that were stained for both *sctU*-op mRNA and *hctA*prom expression as
794 well as non overlapping populations. The *sctU*-op mRNA+ cells were again identified using TrackMate and the
795 signal for *hctA*prom and FISH were quantified for each *sctU*-op+ cell and plotted (magenta dots). Each
796 *hctA*prom+ cell was also identified and the FISH and *hctA*prom signal was determined and plotted (green

797 dots). The *sctU*-op FISH staining was also compared to the expression from the *hctB*prom reporter. The *sctU*-
798 op mRNA FISH staining was again present in a subset of cells but showed little overlap with the *hctB*prom
799 fluorescent signal. The FISH signal and *hctB*prom signal were measured in both cell populations (*sctU* mRNA+
800 cells and *hctB*prom+ cells) and plotted, *sctU* mRNA+ cells magenta dots and *hctB*prom+ cells green dots. Both
801 populations were primary single positive, either *sctU*-op mRNA high or *hctB*rpom high but rarely both. Size bar
802 = 5µm.
803
804 **Figure 8**. Cell type expression of the two T3SS translocons. A) Cos-7 cells were infected with L2-BsciEng for
805 24 hpi and stained for the mRNA expression of the *CTL0238*-op using FISH (magenta), *euo*prom expression
806 (green) and *hctB*prom expression (green). Individual chlamydial cells with *CTL0238*-op mRNA signal from 5
807 separate inclusions were identified using TrackMate and the fluorescence intensity for each channel (mRNA
808 and promoter reporter) was plotted (magenta dots). Individual chlamydial cells positive for *euo*prom, or
809 *hctB*prom signal from 5 separate inclusions were also identified using TrackMate and the expression intensity
810 for each channel (mRNA and promoter reporter) was plotted (green dots). B) Cos-7 cells were infected with L2-
811 BsciEng for 24 hpi and stained for the mRNA expression of the *scc2*-op using FISH. Scc2-op FISH signal in
812 magenta, *euo*prom and *hctB*prom signal in green. Individual chlamydial cells positive for *scc2*-op mRNA signal
813 from 5 inclusions were identified using TrackMate and the fluorescence intensity for each channel (mRNA and
814 promoter reporter) was plotted (magenta dots). Individual chlamydial cells positive for *euo*prom, or *hctB*prom
815 signal from 5 inclusions were also identified using TrackMate and the expression intensity for each channel
816 (mRNA and promoter reporter) was plotted (green dots). Host cells infected with AsciEng and fixed at 16 hpi
817 were probed for *CTL0238*-op mRNA (C) and scc2-op mRNA (D) expression using FISH. *Euo*prom expression
818 (green) had significant overlap with *CTL0238*-op mRNA signal. For the *scc2*-op the FISH signal was
819 undetected. Size bar = 5µm.
820
821 **Figure 9.** Effects of ectopic expression of Euo, HctA, CtcB and HctB on the expression of T3SS effectors.
822 RNA-seq differential expression data (log2fold change) plotted vs the - log of the P value (-log padJ) for *Ctr*
823 ectopically expressing Euo, HctA, CtcB and HctB. **(**A**)** The T3SS effectors are highlighted in purple. (B) All the
824 *inc* protein genes are highlighted in purple while the genes for the *incD-G* operon are highlighted in green, *incV*
825 and *incM* are highlighted in red and orange respectively.
826
827 **Figure 10.** Cell type expression of *incD* and *incV*. Cos-7 cells infected with L2-BsciEng for 16 and 24 hpi and
828 stained for *incD* and *incV* mRNA expression using custom FISH probes. (A) The *incD* mRNA (magenta) was
829 visibly expressed in the *euo*prom+ (green) RB cells at 16 hpi while *hctB*prom signal was not detected. At 24 hpi
830 the *incD* mRNA signal (magenta) overlapped with the *euo*prom signal (green) but was separate from the
831 *hctB*prom+ cells (yellow). (B) The *incV* mRNA signal (magenta) was undetected at 16 hpi. At 24 hpi the *incV*
832 mRNA signal showed overlap with the *hctB*prom signal (yellow) but not the *euo*prom signal (green). C)
833 Individual chlamydial cells positive for *incD* mRNA signal were identified from 5 separate inclusions at 24 hpi
834 using TrackMate and the fluorescence intensity for each channel (mRNA and promoter reporter) was plotted
835 (magenta dots). Individual chlamydial cells positive for *euo*prom, or *hctB*prom signal were also identified using
836 TrackMate and the expression intensity for each channel (mRNA and promoter reporter) was plotted (green
837 dots). D) Individual chlamydial cells positive for *incV* mRNA signal from 5 separate inclusions at 24 hpi were
838 identified using TrackMate and the fluorescence intensity for each channel (mRNA and promoter reporter) was
839 plotted (magenta dots). Individual chlamydial cells positive for *euo*prom or *hctB*prom signal were also identified
840 using TrackMate and the expression intensity for each channel (mRNA and promoter reporter) was plotted
841 (green dots). Size bar = 5µm.
842
843 **Figure 11.** Model of cell type specific deployment of the T3SS. In this model the *scc2*-op translocon secretes
844 effectors across the plasma membrane (PM) for host cell entry. The *scc2*-op translocon is replaced in the RB
845 with the *CTL0239*-op translocon for the secretion of the Inc proteins across the inclusion membrane (IM). The

846 structural components of the T3SS are then reconstructed during the IB to EB maturation phase. The Euo+,
847 HctA+, CtcB+ and HctB+ nomenclature indicates in which cell form the protein is active.
848
849 Supplemental table legends
850 Table S1. Chlamydial genes designated as RB, IB, EB expressed genes and their regulation from ectopic
851 expression of Euo, HctA, CtcB and HctB. Gene expression time categories: Immediate early genes, Mid-late
852 genes and Late genes from Soules et al and Belland et al. Serovar D annotation included just for reference
853 and does not indicate experimentally measured values.
854
855 Table S2. T3SS structural operons.
856
857 Table S3. T3SS effector gene regulation from ectopic expression of Euo, HctA, CtcB and HctB. Serovar D
858 annotation included for reference and does not indicate experimentally measured values.
859
860 Table S4. Inc gene regulation from ectopic expression of Euo, HctA, CtcB and HctB. Serovar D annotation
861 included just for reference and does not indicate experimentally measured values.
862
863 Table S5. List of primers used to construct plasmids
864
865 Table S6. List of FISH probes and the location on the Ctr genome

References:

1. Abdelrahman, Y.M., and Belland, R.J. (2005). The chlamydial developmental cycle. FEMS Microbiol. Rev. *29*, 949–959. https://doi.org/10.1016/J.FEMSRE.2005.03.002.
2. Rockey, D.D., and Matsumoto, A. (2000). The chlamydial developmental cycle. Prokaryotic Dev., 403–425.
3. Bakken, I.J. (2007). Chlamydia trachomatis Infection and the Risk for Ectopic Pregnancy. Sex. Transm. Dis. *34*. https://doi.org/10.1097/01.OLQ.0000253171.99295.48.
4. Ohman, H., Tiitinen, A., Halttunen, M., Lehtinen, M., Paavonen, J., and Surcel, H.-M. Cytokine polymorphisms and severity of tubal damage in women with Chlamydia-associated infertility. J. Infect. Dis. *199*, 1353–1359. https://doi.org/10.1086/597620.
5. Reekie, J., Donovan, B., Guy, R., Hocking, J.S., Kaldor, J.M., Mak, D., Preen, D., Ward, J., Liu, B., and Chlamydia and Reproductive Health Outcome Investigators (2019). Risk of Ectopic Pregnancy and Tubal Infertility Following Gonorrhea and Chlamydia Infections. Clin. Infect. Dis. *69*, 1621–1623. https://doi.org/10.1093/cid/ciz145.
6. Schachter, J. (1988). Chlamydiaceae: The Chlamydiae. In, pp. 847–863. https://doi.org/10.1007/978-1-4612-3900-0_43.
7. Everett, K.D., Bush, R.M., and Andersen, A.A. (1999). Emended description of the order Chlamydiales, proposal of Parachlamydiaceae fam. nov. and Simkaniaceae fam. nov., each containing one monotypic genus, revised taxonomy of the family Chlamydiaceae, including a new genus and five new species, and standards for the identification of organisms. Int. J. Syst. Evol. Microbiol. *49 Pt 2*, 415–440. https://doi.org/10.1099/00207713-49-2-415.
8. Chiarelli, T.J., Grieshaber, N.A., Omsland, A., Remien, C.H., and Grieshaber, S.S. (2020). Single-Inclusion Kinetics of Chlamydia trachomatis Development. MSystems *5*. https://doi.org/10.1128/MSYSTEMS.00689-20.
9. Chiarelli, T.J., Grieshaber, N.A., Appa, C.R., and Grieshaber, S.S. (2023). Computational Modeling of the Chlamydial Developmental Cycle Reveals a Potential Role for Asymmetric Division. mSystems *8*, e00053-23. https://doi.org/10.1128/msystems.00053-23.
10. Clifton, D.R., Dooley, C.A., Grieshaber, S.S., Carabeo, R.A., Fields, K.A., and Hackstadt, T. (2005). Tyrosine phosphorylation of the chlamydial effector protein Tarp is species specific and not required for recruitment of actin. Infect. Immun. *73*, 3860–3868. https://doi.org/10.1128/IAI.73.7.3860-3868.2005.
11. Chen, Y.-S., Bastidas, R.J., Saka, H.A., Carpenter, V.K., Richards, K.L., Plano, G.V., and Valdivia, R.H. (2014). The Chlamydia trachomatis type III secretion chaperone Slc1 engages multiple early effectors, including TepP, a tyrosine-phosphorylated protein required for the recruitment of CrkI-II to nascent inclusions and innate immune signaling. PLoS Pathog. *10*. https://doi.org/10.1371/JOURNAL.PPAT.1003954.
12. Abdelrahman, Y., Ouellette, S.P., Belland, R.J., and Cox, J.V. (2016). Polarized Cell Division of Chlamydia trachomatis. PLoS Pathog. *12*. https://doi.org/10.1371/JOURNAL.PPAT.1005822.
13. Wurihan, W., Zou, Y., Weber, A.M., Weldon, K., Huang, Y., Bao, X., Zhu, C., Wu, X., Wang, Y., Lai, Z., et al. (2021). Identification of a GrgA-Euo-HrcA Transcriptional Regulatory Network in Chlamydia. mSystems *6*, e0073821. https://doi.org/10.1128/mSystems.00738-21.
14. Belland, R.J., Zhong, G., Crane, D.D., Hogan, D., Sturdevant, D., Sharma, J., Beatty, W.L., and Caldwell, H.D. (2003). Genomic transcriptional profiling of the developmental cycle of Chlamydia trachomatis. Proc. Natl. Acad. Sci. *100*, 8478–8483. https://doi.org/10.1073/PNAS.1331135100.
15. Shaw, E.I., Dooley, C.A., Fischer, E.R., Scidmore, M.A., Fields, K.A., and Hackstadt, T. Three temporal classes of gene expression during the Chlamydia trachomatis developmental cycle. Mol. Microbiol. *37*, 913–925.
16. Nicholson, T.L., Olinger, L., Chong, K., Schoolnik, G., and Stephens, R.S. (2001). Global Stage-Specific Gene Regulation during the Developmental Cycle of Chlamydia trachomatis. J. Bacteriol. *185*, 3179–3189. https://doi.org/10.1128/JB.185.10.3179-3189.2003.
17. Hakiem, O.R., Rizvi, S.M.A., Ramirez, C., and Tan, M. Euo is a developmental regulator that represses late

genes and activates midcycle genes in *Chlamydia trachomatis*. mBio *0*, e00465-23. https://doi.org/10.1128/mbio.00465-23.
18. Rosario, C.J., Hanson, B.R., and Tan, M. The transcriptional repressor EUO regulates both subsets of Chlamydia late genes. Mol. Microbiol. *94*, 888–897. https://doi.org/10.1111/mmi.12804.
19. Barry, C.E., Brickman, T.J., and Hackstadt, T. (1990). Hc1-mediated effects on DNA structure: a potential regulator of chlamydial development. Mol. Microbiol. *9*, 273–283. https://doi.org/10.1111/j.1365-2958.1993.tb01689.x.
20. Grieshaber, N.A., Grieshaber, S.S., Fischer, E.R., and Hackstadt, T. A small RNA inhibits translation of the histone-like protein Hc1 in Chlamydia trachomatis. Mol. Microbiol. *59*, 541–550. https://doi.org/10.1111/j.1365-2958.2005.04949.x.
21. Grieshaber, N.A., Fischer, E.R., Mead, D.J., Dooley, C.A., and Hackstadt, T. (2004). Chlamydial histone-DNA interactions are disrupted by a metabolite in the methylerythritol phosphate pathway of isoprenoid biosynthesis. Proc. Natl. Acad. Sci. U. S. A. *101*, 7451—7456. https://doi.org/10.1073/pnas.0400754101.
22. Brickman, T.J., Barry, C.E. 3rd, and Hackstadt, T. (1991). Molecular cloning and expression of hctB encoding a strain-variant chlamydial histone-like protein with DNA-binding activity. J. Bacteriol. *175*.
23. Koo, I.C., and Stephens, R.S. (2003). A developmentally regulated two-component signal transduction system in Chlamydia. J. Biol. Chem. *278*, 17314–17319. https://doi.org/10.1074/JBC.M212170200.
24. Soules, K.R., LaBrie, S.D., May, B.H., and Hefty, P.S. (2020). Sigma 54-Regulated Transcription Is Associated with Membrane Reorganization and Type III Secretion Effectors during Conversion to Infectious Forms of Chlamydia trachomatis. MBio *11*. https://doi.org/10.1128/MBIO.01725-20.
25. Grieshaber, N.A., Chiarelli, T.J., Appa, C.R., Neiswanger, G., Peretti, K., and Grieshaber, S.S. (2022). Translational gene expression control in Chlamydia trachomatis. PLoS ONE *17*. https://doi.org/10.1371/JOURNAL.PONE.0257259.
26. Waskom, M.L. (2021). seaborn: statistical data visualization. J. Open Source Softw. *6*, 3021. https://doi.org/10.21105/joss.03021.
27. Hatch Nathan D. and Ouellette Scot P. (2023). Identification of the alternative sigma factor regulons of Chlamydia trachomatis using multiplexed CRISPR interference. mSphere *8*, e00391-23. https://doi.org/10.1128/msphere.00391-23.
28. Tinevez, J.-Y., Perry, N., Schindelin, J., Hoopes, G.M., Reynolds, G.D., Laplantine, E., Bednarek, S.Y., Shorte, S.L., and Eliceiri, K.W. (2014). TrackMate: An open and extensible platform for single-particle tracking. Methods *115*, 80–90. https://doi.org/10.1016/j.ymeth.2016.09.016.
29. Kubo, A., and Stephens, R.S. (2000). Characterization and functional analysis of PorB, a Chlamydia porin and neutralizing target. Mol. Microbiol. *38*, 772–780. https://doi.org/10.1046/J.1365-2958.2000.02167.X.
30. Grieshaber, S., Grieshaber, N., Yang, H., Baxter, B., Hackstadt, T., and Omsland, A. (2018). Impact of Active Metabolism on Chlamydia trachomatis Elementary Body Transcript Profile and Infectivity. J. Bacteriol. *200*. https://doi.org/10.1128/JB.00065-18.
31. Price, M.N., Huang, K.H., Alm, E.J., and Arkin, A.P. (2005). A novel method for accurate operon predictions in all sequenced prokaryotes. Nucleic Acids Res. *33*, 880–892. https://doi.org/10.1093/nar/gki232.
32. Hefty, P.S., and Stephens, R.S. (2007). Chlamydial type III secretion system is encoded on ten operons preceded by sigma 70-like promoter elements. J. Bacteriol. *189*, 198–206. https://doi.org/10.1128/JB.01034-06.
33. Stephens, R.S., Kalman, S., Lammel, C., Fan, J., Marathe, R., Aravind, L., Mitchell, W., Olinger, L., Tatusov, R.L., Zhao, Q., et al. (1998). Genome sequence of an obligate intracellular pathogen of humans: Chlamydia trachomatis. Science *282*, 754–759. https://doi.org/10.1126/SCIENCE.282.5389.754.
34. Dey, S., Chakravarty, A., Guha Biswas, P., and De Guzman, R.N. (2019). The type III secretion system needle, tip, and translocon. Protein Sci. Publ. Protein Soc. *28*, 1582–1593. https://doi.org/10.1002/pro.3682.
35. Betts-Hampikian, H.J., and Fields, K.A. (2010). The Chlamydial Type III Secretion Mechanism: Revealing Cracks in a Tough Nut. Front. Microbiol. *1*. https://doi.org/10.3389/FMICB.2010.00114.
36. Dehoux, P., Flores, R., Dauga, C., Zhong, G., and Subtil, A. Multi-genome identification and

966 characterization of chlamydiae-specific type III secretion substrates: the Inc proteins. BMC Genomics *12*.
967 https://doi.org/10.1186/1471-2164-12-109.
968 37. Peters, J., Wilson, D.P., Myers, G., Timms, P., and Bavoil, P.M. (2005). Type III secretion à la Chlamydia.
969 Trends Microbiol. *15*, 241–251. https://doi.org/10.1016/j.tim.2007.04.005.
970 38. Ferrell, J.C., and Fields, K.A. A working model for the type III secretion mechanism in Chlamydia.
971 Microbes Infect. Inst. Pasteur *18*, 84–92. https://doi.org/10.1016/j.micinf.2015.10.006.
972 39. Lutter, E.I., Martens, C., and Hackstadt, T. Evolution and conservation of predicted inclusion membrane
973 proteins in chlamydiae. Comp. Funct. Genomics *2012*. https://doi.org/10.1155/2012/362104.
974 40. Rockey, D.D., Scidmore, M.A., Bannantine, J.P., and Brown, W.J. (2002). Proteins in the chlamydial
975 inclusion membrane. Microbes Infect. *4*, 333–340. https://doi.org/10.1016/S1286-4579(02)01546-0.
976 41. Stanhope, R., Flora, E., Bayne, C., and Derré, I. (2017). IncV, a FFAT motif-containing Chlamydia protein,
977 tethers the endoplasmic reticulum to the pathogen-containing vacuole. Proc. Natl. Acad. Sci. *114*, 12039–
978 12044. https://doi.org/10.1073/PNAS.1709060114.
979 42. Luís, M.P., Pereira, I.S., Bugalhão, J.N., Simões, C.N., Mota, C., Romão, M.J., and Mota, L.J. (2023). The
980 Chlamydia trachomatis IncM Protein Interferes with Host Cell Cytokinesis, Centrosome Positioning, and
981 Golgi Distribution and Contributes to the Stability of the Pathogen-Containing Vacuole. Infect. Immun. *91*,
982 e0040522. https://doi.org/10.1128/iai.00405-22.
983 43. Wilson, D.P., Timms, P., McElwain, D.L.S., and Bavoil, P.M. (2006). Type III secretion, contact-dependent
984 model for the intracellular development of chlamydia. Bull. Math. Biol. *68*, 161–178.
985 https://doi.org/10.1007/s11538-005-9024-1.
986 44. Hoare, A., Timms, P., Bavoil, P.M., and Wilson, D.P. (2006). Spatial constraints within the chlamydial host
987 cell inclusion predict interrupted development and persistence. BMC Microbiol. *8*.
988 https://doi.org/10.1186/1471-2180-8-5.
989 45. Grieshaber, N.A., Runac, J., Turner, S., Dean, M., Appa, C., Omsland, A., and Grieshaber, S.S. (2021). The
990 sRNA Regulated Protein DdbA Is Involved in Development and Maintenance of the Chlamydia trachomatis
991 EB Cell Form. Front. Cell. Infect. Microbiol. *11*. https://doi.org/10.3389/FCIMB.2021.692224.
992 46. Shen Li, Gao Leiqiong, Swoboda Abigail R., and Ouellette Scot P. (2024). Targeted repression of topA by
993 CRISPRi reveals a critical function for balanced DNA topoisomerase I activity in the Chlamydia
994 trachomatis developmental cycle. mBio *15*, e02584-23. https://doi.org/10.1128/mbio.02584-23.
995 47. Niehus, E., Cheng, E., and Tan, M. (2008). DNA supercoiling-dependent gene regulation in Chlamydia. J.
996 Bacteriol. *190*, 6419–6427. https://doi.org/10.1128/JB.00431-08.
997 48. Cheng Eric and Tan Ming (2012). Differential Effects of DNA Supercoiling on Chlamydia Early Promoters
998 Correlate with Expression Patterns in Midcycle. J. Bacteriol. *194*, 3109–3115.
999 https://doi.org/10.1128/jb.00242-12.
000 49. Howard, L., Orenstein, N.S., and King, N.W. (1970). Purification on renografin density gradients of
001 Chlamydia trachomatis grown in the yolk sac of eggs. Appl. Microbiol. *27*, 102–106.
002 50. Derré, I., Swiss, R., and Agaisse, H. (2011). The lipid transfer protein CERT interacts with the Chlamydia
003 inclusion protein IncD and participates to ER-Chlamydia inclusion membrane contact sites. PLoS Pathog. *7*.
004 https://doi.org/10.1371/JOURNAL.PPAT.1002092.
005 51. Langmead, B., and Salzberg, S.L. (2012). Fast gapped-read alignment with Bowtie 2. Nat. Methods *9*, 357–
006 359. https://doi.org/10.1038/nmeth.1923.
007 52. Love, M.I., Huber, W., and Anders, S. (2012). Moderated estimation of fold change and dispersion for
008 RNA-seq data with DESeq2. Genome Biol *15*. https://doi.org/10.1186/s13059-014-0550-8.
009 53. Shukla, X.U., and Parmar, D.J. (2014). Python – A comprehensive yet free programming language for
010 statisticians. J. Stat. Manag. Syst. *19*, 277–284. https://doi.org/10.1080/09720510.2015.1103446.

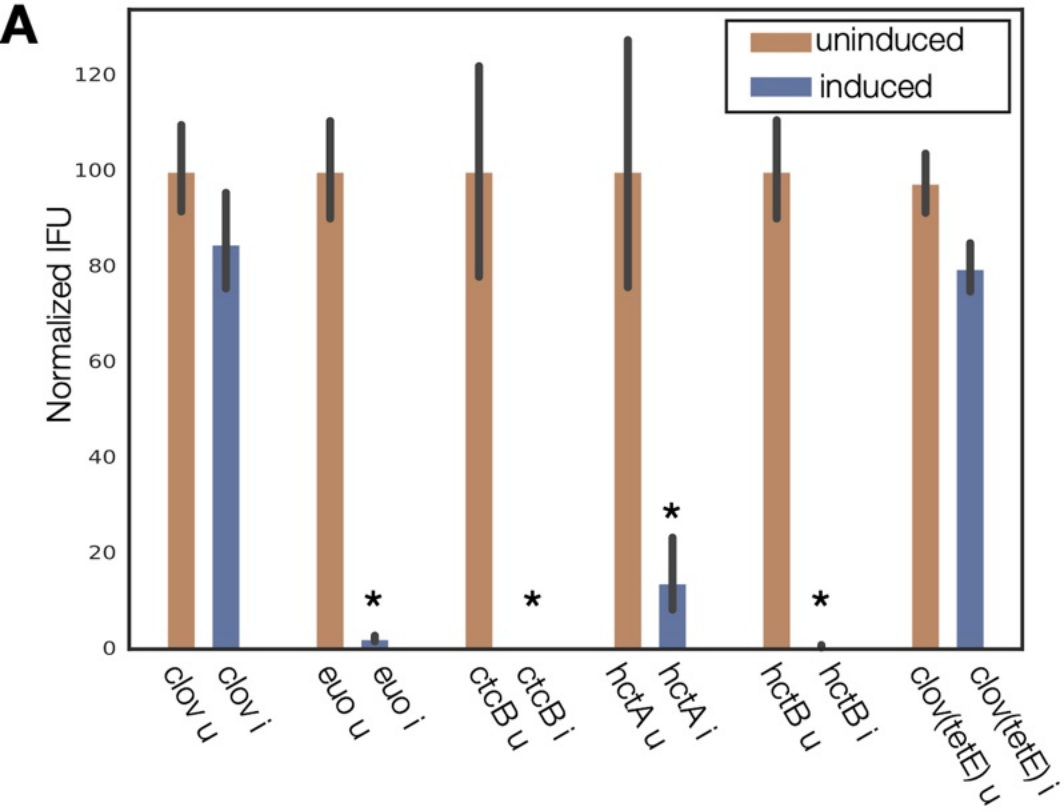
A
uninduced
induced
Normalized IFU
0
20
40
60
80
100
120
clov u
clov i
euo u
euo i
ctcB u
ctcB i
hctA u
hctA i
hctB u
hctB i
clov(tetE) u
clov(tetE) i

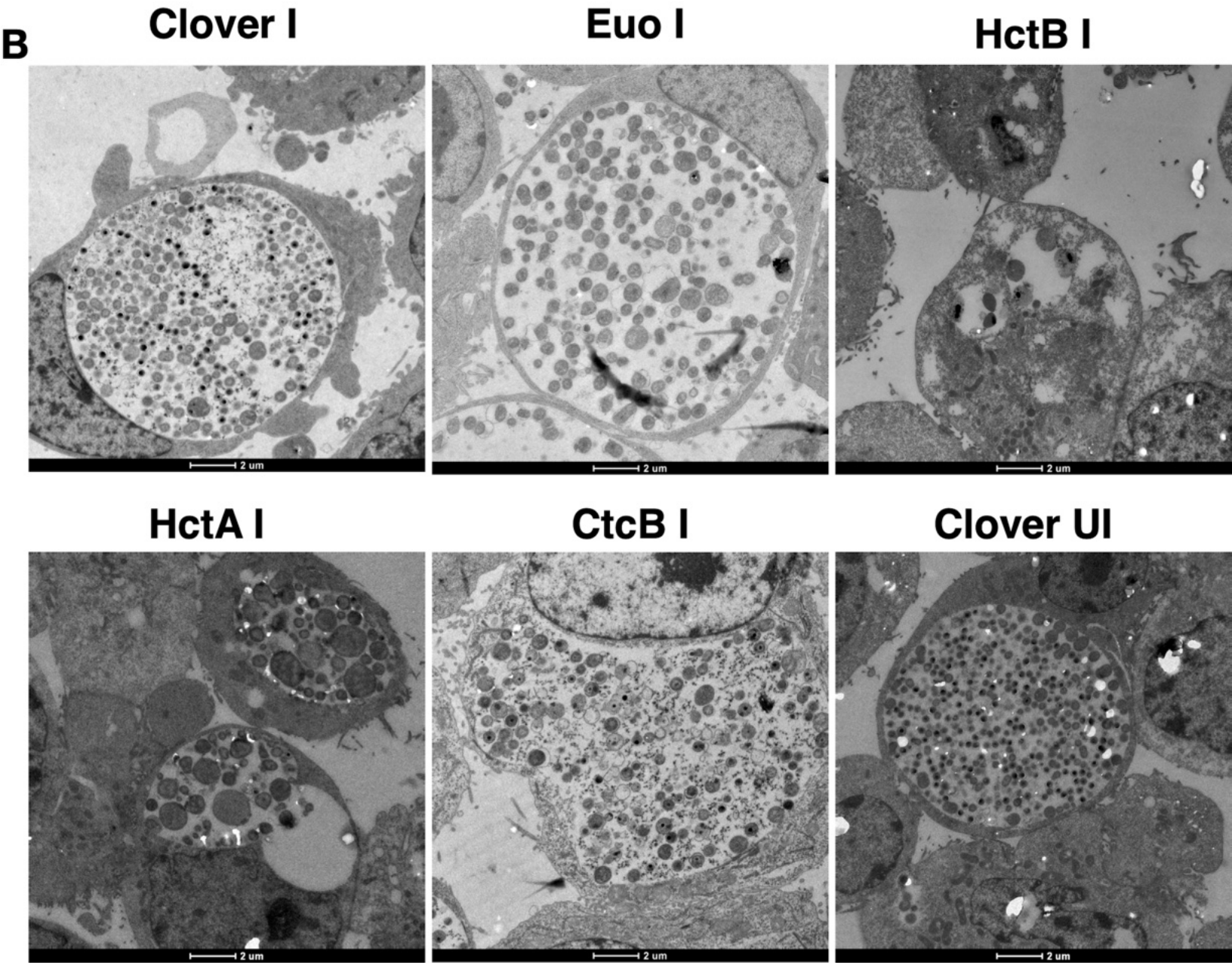
B
Clover I
Euo I
HctB I
HctA I
CtcB I
Clover UI
2 um

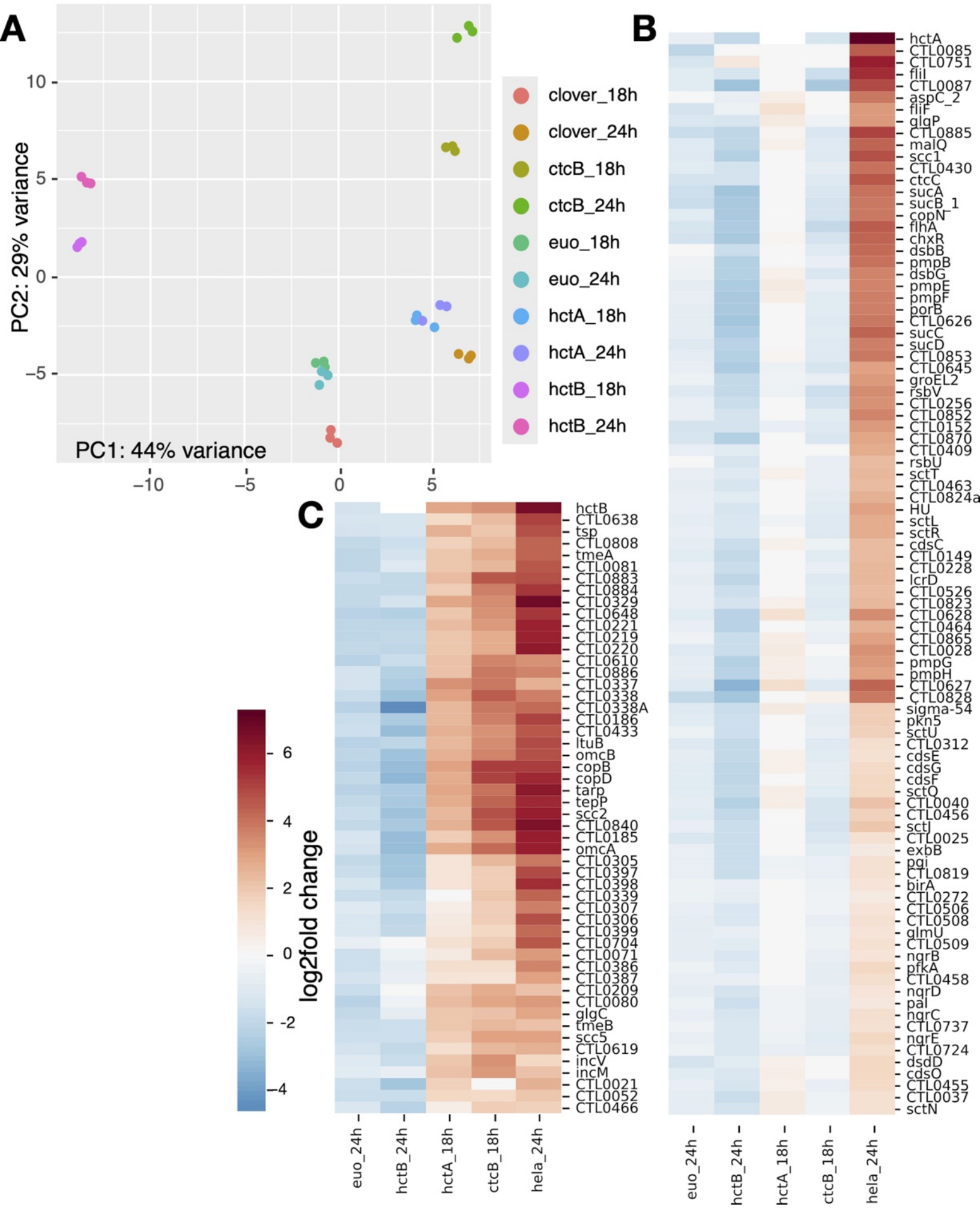
A
PC2: 29% variance
PC1: 44% variance
10
5
0
−5
−10
−5
0
5
clover_18h
clover_24h
ctcB_18h
ctcB_24h
euo_18h
euo_24h
hctA_18h
hctA_24h
hctB_18h
hctB_24h
B
hctA
CTL0085
CTL0751
fliI
CTL0087
aspC_2
fliF
glgP
CTL0885
malQ
scc1
CTL0430
ctcC
sucA
sucB_1
copN
flhA
chxR
dsbB
pmpB
dsbG
pmpE
pmpF
porB
CTL0626
sucC
sucD
CTL0853
CTL0645
groEL2
rsbV
CTL0256
CTL0852
CTL0152
CTL0870
CTL0409
rsbU
sctT
CTL0463
CTL0824a
HU
sctL
sctR
cdsC
CTL0149
CTL0228
lcrD
CTL0526
CTL0823
CTL0628
CTL0464
CTL0865
CTL0028
pmpG
pmpH
CTL0627
CTL0828
sigma-54
pkn5
sctU
CTL0312
cdsE
cdsG
cdsF
sctQ
CTL0040
CTL0456
sctJ
CTL0025
exbB
pgi
CTL0819
birA
CTL0272
CTL0506
CTL0508
glmU
CTL0509
nqrB
pfkA
CTL0458
nqrD
pal
nqrC
CTL0737
nqrE
CTL0724
dsdD
cdsO
CTL0455
CTL0037
sctN
euo_24h
hctB_24h
hctA_18h
ctcB_18h
hela_24h
C
hctB
CTL0638
tsp
CTL0808
tmeA
CTL0081
CTL0883
CTL0884
CTL0329
CTL0648
CTL0221
CTL0219
CTL0220
CTL0610
CTL0886
CTL0337
CTL0338
CTL0338A
CTL0186
CTL0433
ltuB
omcB
copB
copD
tarp
tepP
scc2
CTL0840
CTL0185
omcA
CTL0305
CTL0397
CTL0398
CTL0339
CTL0307
CTL0306
CTL0399
CTL0704
CTL0071
CTL0386
CTL0387
CTL0209
CTL0080
glgC
tmeB
scc5
CTL0619
incV
incM
CTL0021
CTL0052
CTL0466
log2fold change
6
4
2
0
-2
−4
euo_24h
hctB_24h
hctA_18h
ctcB_18h
hela_24h

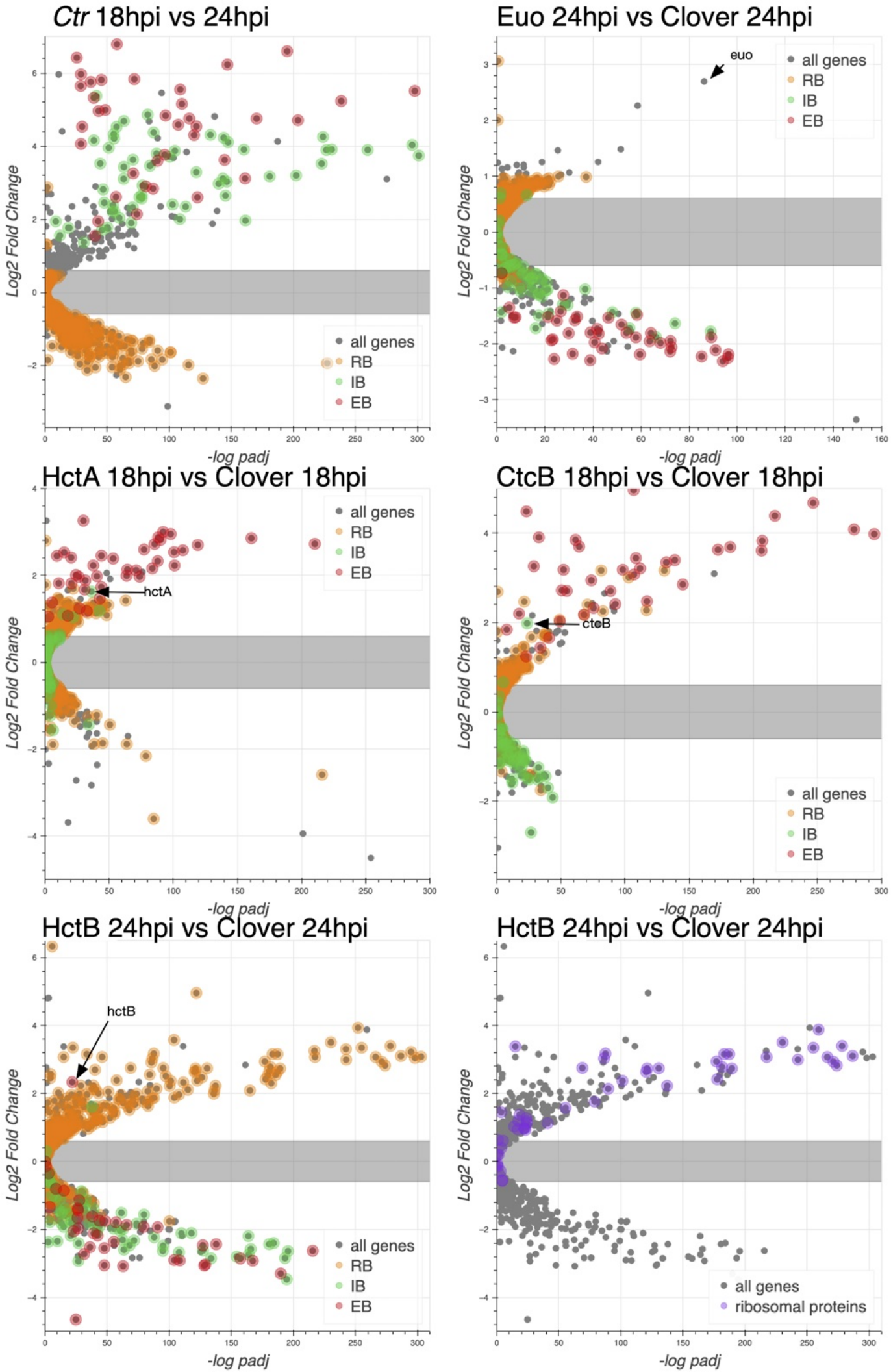
Ctr 18hpi vs 24hpi
Euo 24hpi vs Clover 24hpi
HctA 18hpi vs Clover 18hpi
CtcB 18hpi vs Clover 18hpi
HctB 24hpi vs Clover 24hpi
HctB 24hpi vs Clover 24hpi
Log2 Fold Change
-log padj
all genes
RB
IB
EB
ribosomal proteins
euo
hctA
ctcB
hctB

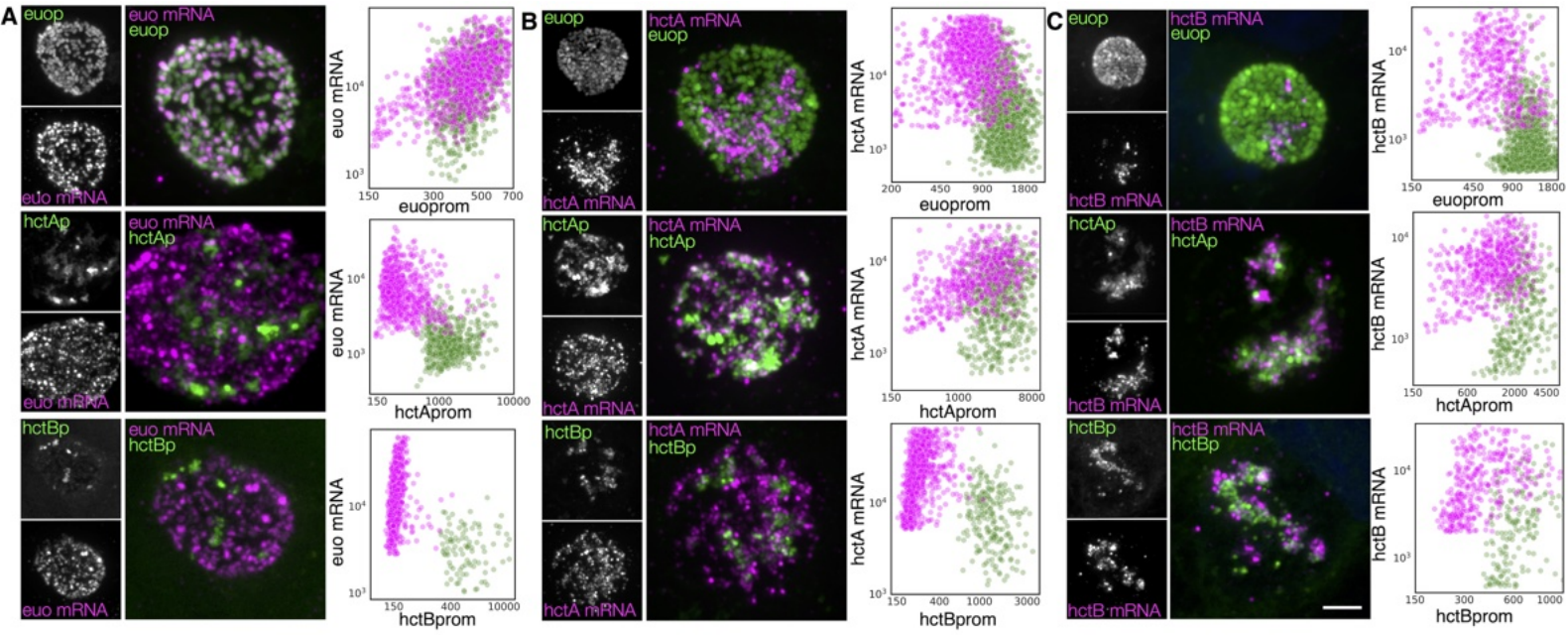
A
euop
euo mRNA
euo mRNA
euop
euo mRNA
euoprom
hctAp
euo mRNA
hctAp
euo mRNA
hctAprom
hctBp
euo mRNA
hctBp
euo mRNA
hctBprom
B
euop
hctA mRNA
hctA mRNA
euop
hctA mRNA
euoprom
hctAp
hctA mRNA
hctAp
hctA mRNA
hctAprom
hctBp
hctA mRNA
hctBp
hctA mRNA
hctBprom
C
euop
hctB mRNA
hctB mRNA
euop
hctB mRNA
euoprom
hctAp
hctB mRNA
hctAp
hctB mRNA
hctAprom
hctBp
hctB mRNA
hctBp
hctB mRNA
hctBprom

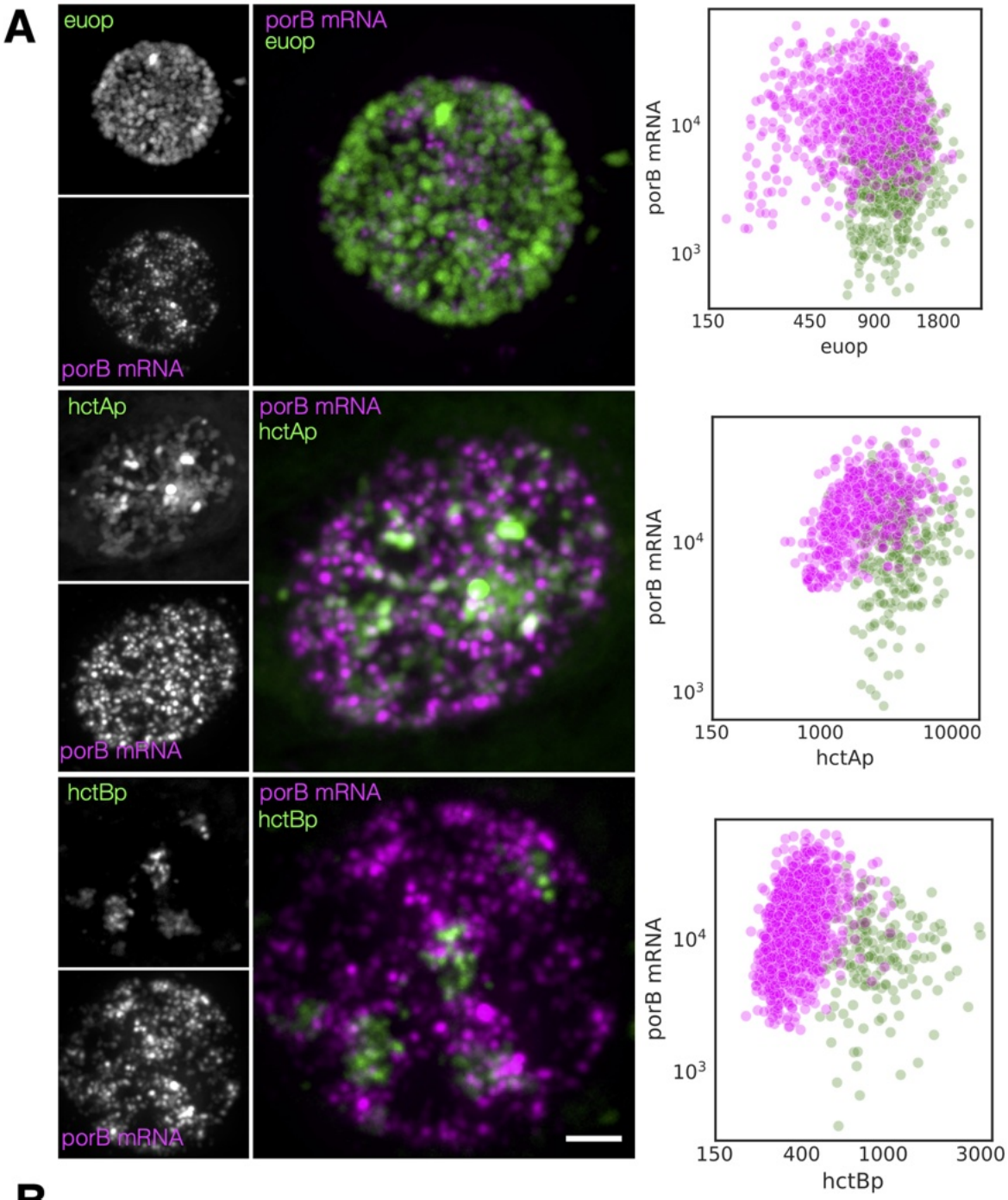
A
euop
porB mRNA
porB mRNA
euop
porB mRNA
euop
hctAp
porB mRNA
porB mRNA
hctAp
porB mRNA
hctAp
hctBp
porB mRNA
porB mRNA
hctBp
porB mRNA
hctBp
porB mRNA
10^4
10^3
150
450
900
1800
euop
porB mRNA
10^4
10^3
150
1000
10000
hctAp
porB mRNA
10^4
10^3
150
400
1000
3000
hctBp

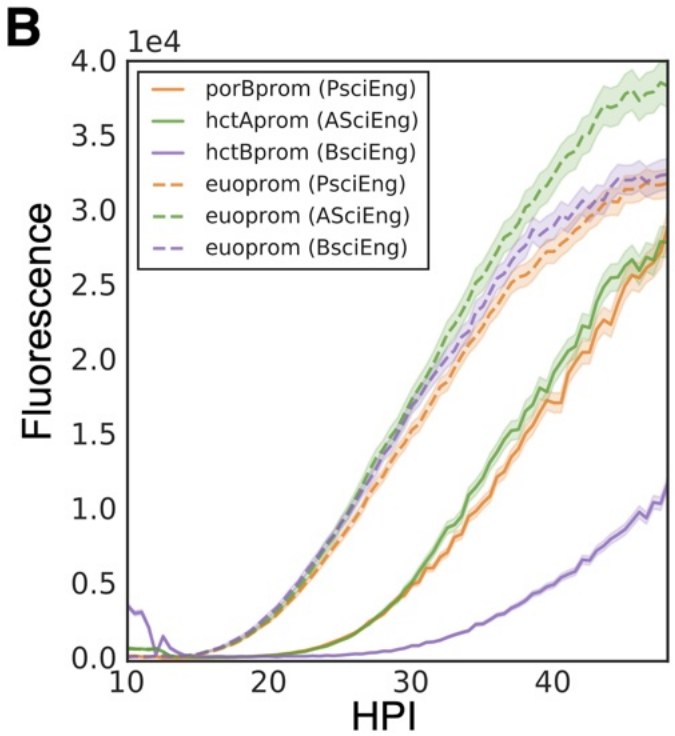
B
1e4
4.0
3.5
3.0
2.5
2.0
1.5
1.0
0.5
0.0
Fluorescence
porBprom (PsciEng)
hctAprom (ASciEng)
hctBprom (BsciEng)
euoprom (PsciEng)
euoprom (ASciEng)
euoprom (BsciEng)
10
20
30
40
HPI

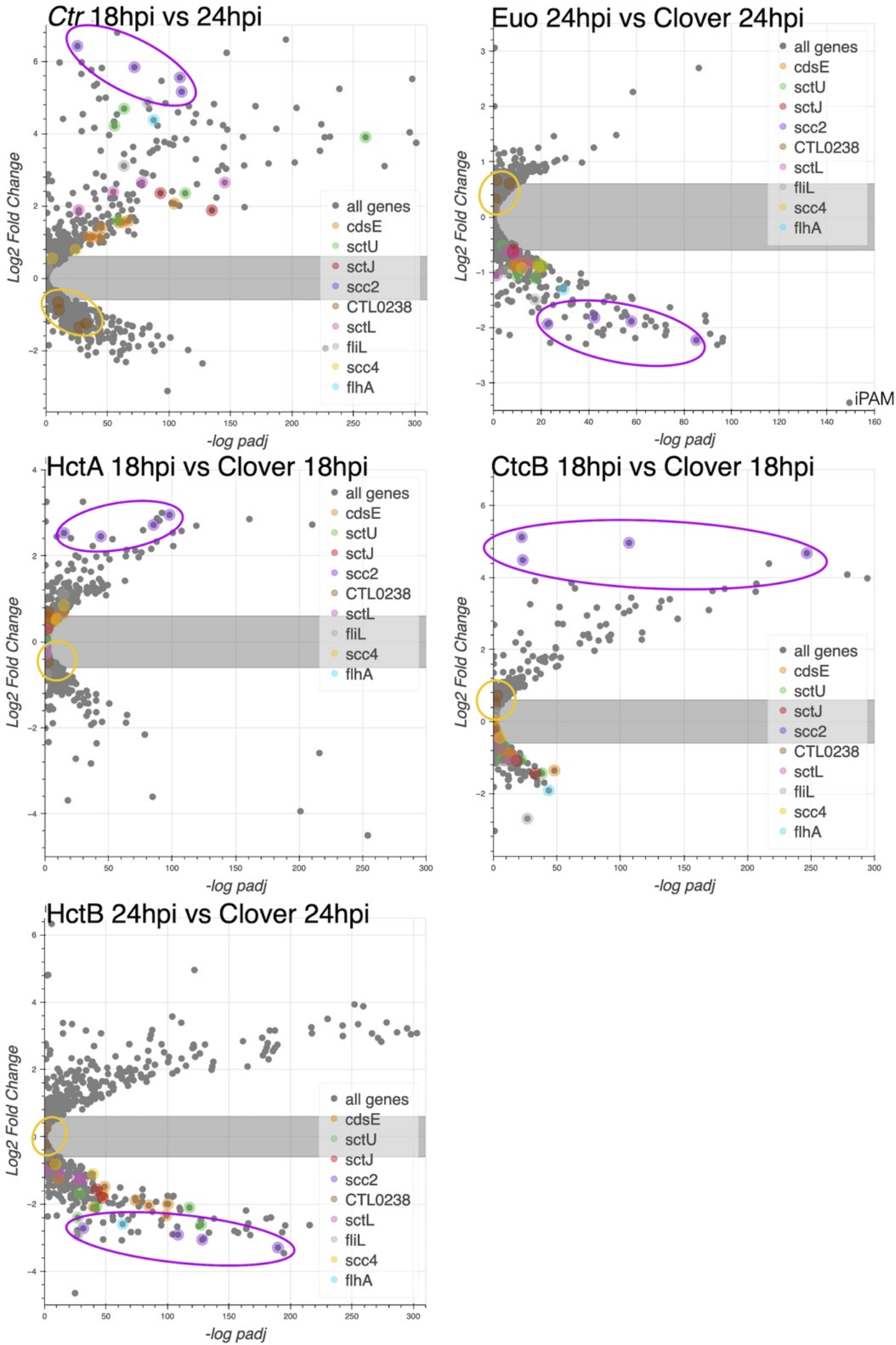
Ctr 18hpi vs 24hpi
Euo 24hpi vs Clover 24hpi
HctA 18hpi vs Clover 18hpi
CtcB 18hpi vs Clover 18hpi
HctB 24hpi vs Clover 24hpi
Log2 Fold Change
-log padj
all genes
cdsE
sctU
sctJ
scc2
CTL0238
sctL
fliL
scc4
flhA
iPAM

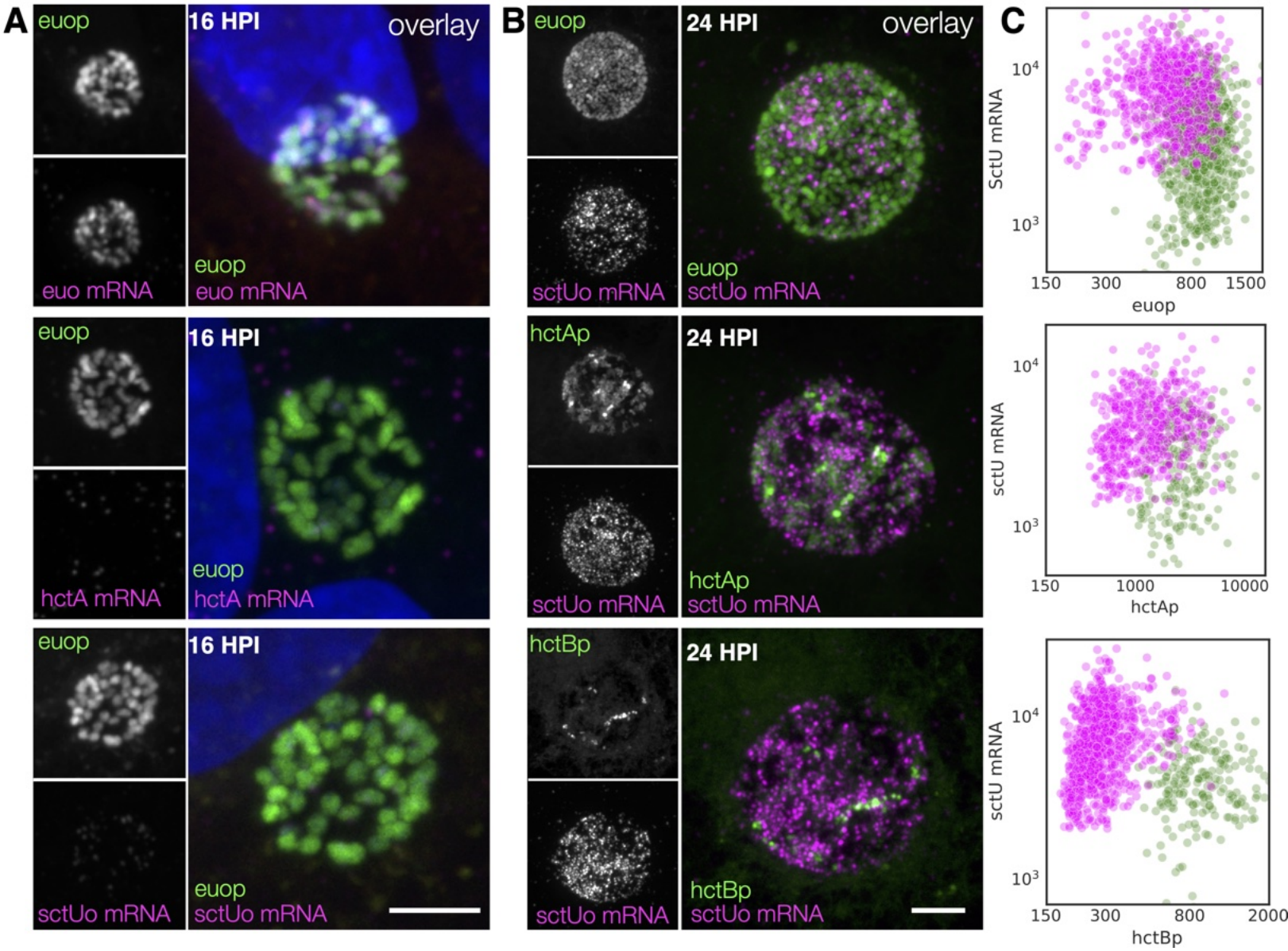
A
euop
euo mRNA
16 HPI
overlay
euop
euo mRNA
euop
hctA mRNA
16 HPI
euop
hctA mRNA
euop
sctUo mRNA
16 HPI
euop
sctUo mRNA
B
euop
sctUo mRNA
24 HPI
overlay
euop
sctUo mRNA
hctAp
sctUo mRNA
24 HPI
hctAp
sctUo mRNA
hctBp
sctUo mRNA
24 HPI
hctBp
sctUo mRNA
C
SctU mRNA
euop
sctU mRNA
hctAp
sctU mRNA
hctBp

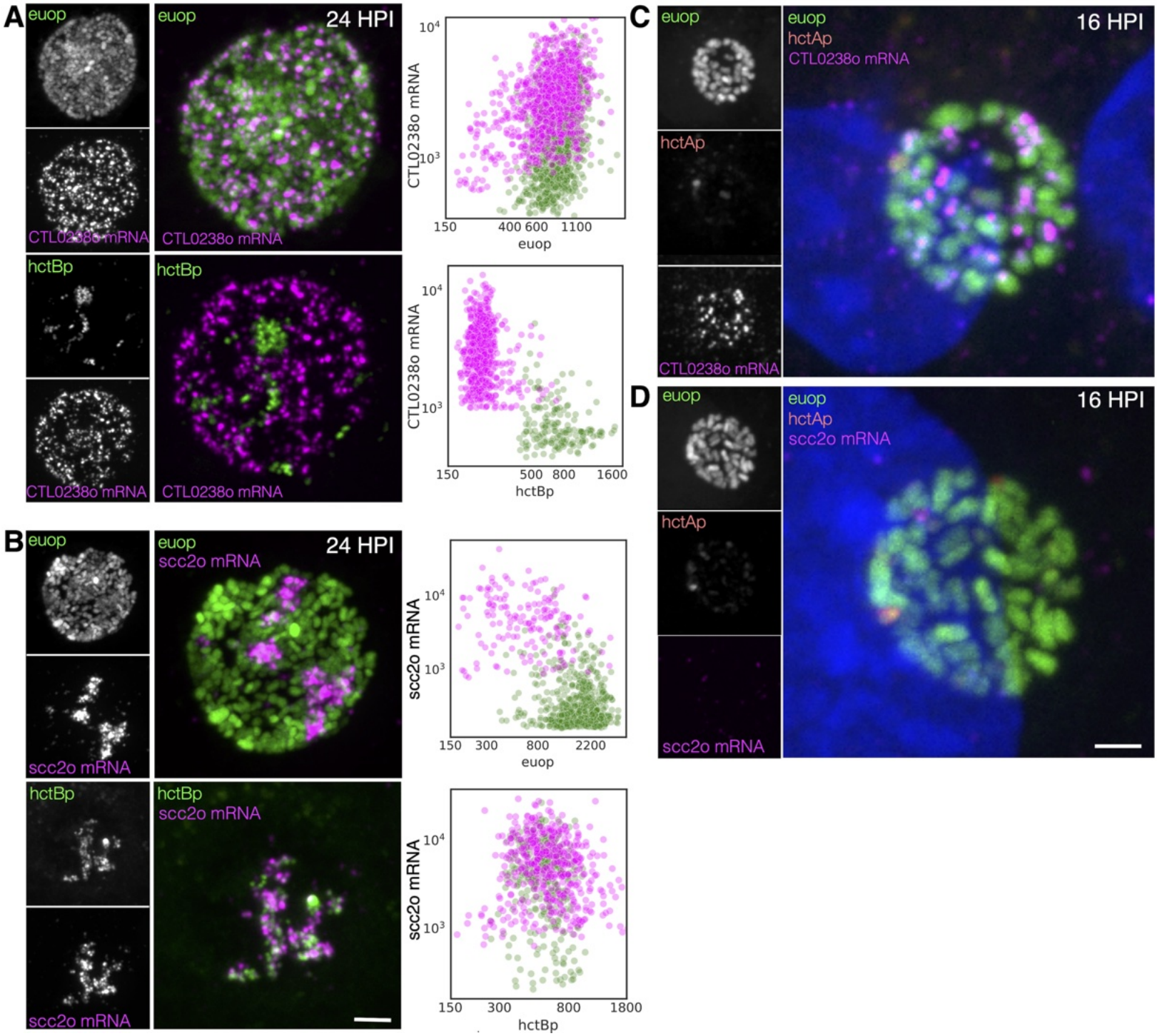
A
euop
CTL0238o mRNA
hctBp
CTL0238o mRNA
euop
24 HPI
CTL0238o mRNA
hctBp
CTL0238o mRNA
CTL0238o mRNA
euop
150
400 600
1100
CTL0238o mRNA
hctBp
150
500 800
1600
B
euop
scc2o mRNA
hctBp
scc2o mRNA
euop
scc2o mRNA
24 HPI
hctBp
scc2o mRNA
scc2o mRNA
euop
150 300
800
2200
scc2o mRNA
hctBp
150
300
800
1800
C
euop
hctAp
CTL0238o mRNA
euop
hctAp
CTL0238o mRNA
16 HPI
D
euop
hctAp
scc2o mRNA
euop
hctAp
scc2o mRNA
16 HPI

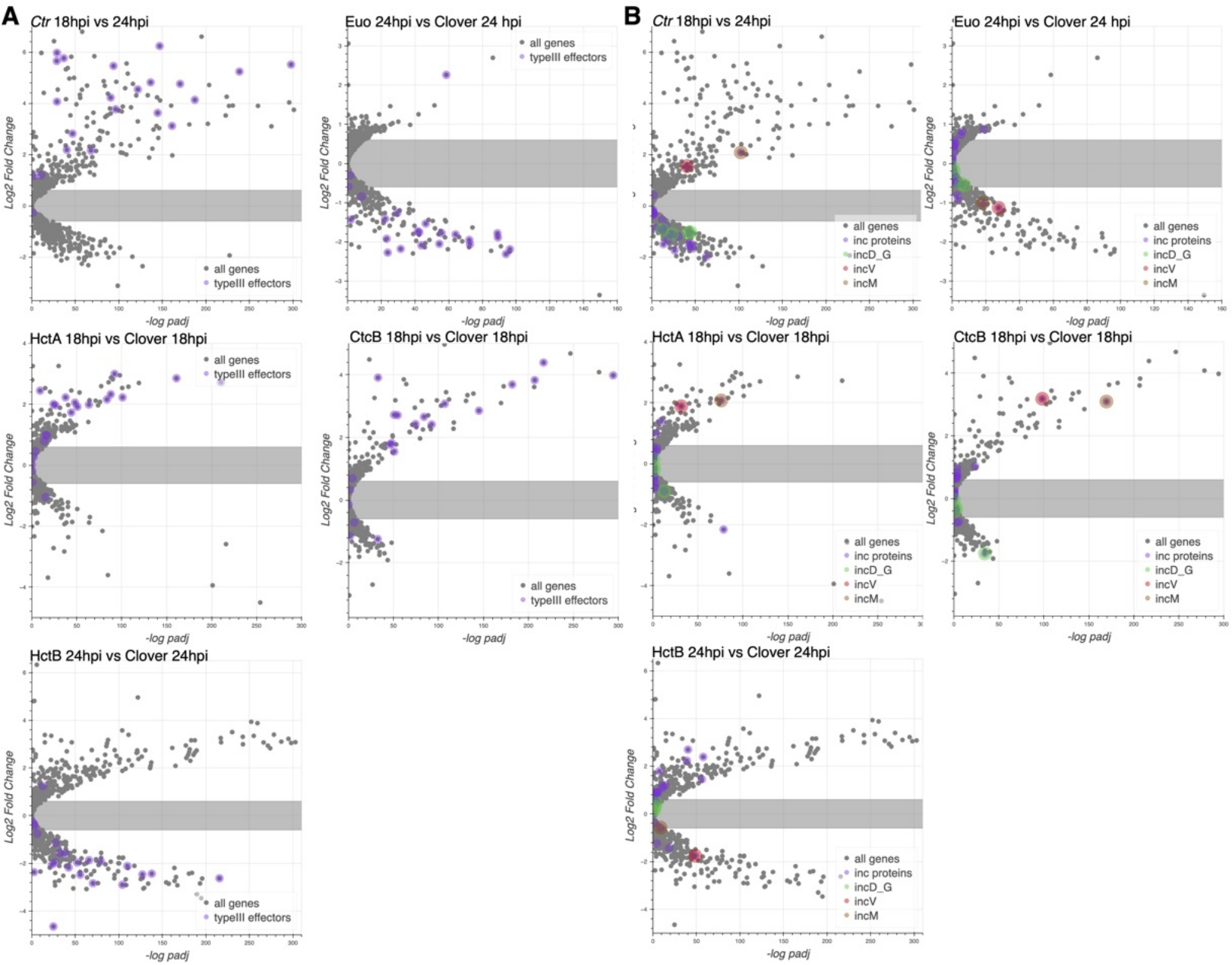
A
Ctr 18hpi vs 24hpi
Euo 24hpi vs Clover 24 hpi
HctA 18hpi vs Clover 18hpi
CtcB 18hpi vs Clover 18hpi
HctB 24hpi vs Clover 24hpi
B
Ctr 18hpi vs 24hpi
Euo 24hpi vs Clover 24 hpi
HctA 18hpi vs Clover 18hpi
CtcB 18hpi vs Clover 18hpi
HctB 24hpi vs Clover 24hpi
Log2 Fold Change
-log padj
all genes
typeIII effectors
inc proteins
incD_G
incV
incM

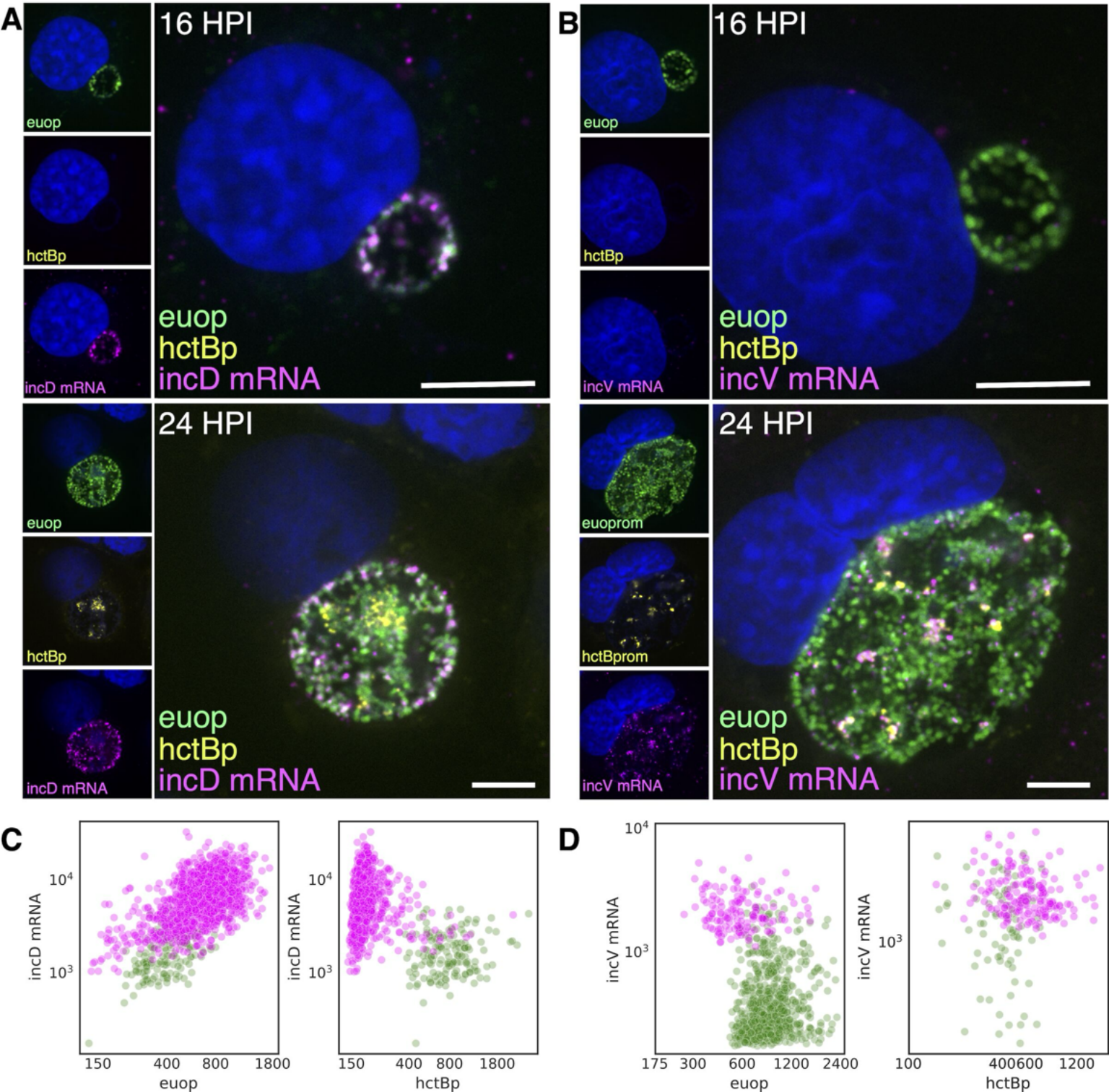
A
16 HPI
euop
hctBp
incD mRNA
euop
hctBp
incD mRNA
24 HPI
euop
hctBp
incD mRNA
euop
hctBp
incD mRNA
B
16 HPI
euop
hctBp
incV mRNA
euop
hctBp
incV mRNA
24 HPI
euoprom
hctBprom
incV mRNA
euop
hctBp
incV mRNA
C
incD mRNA
10^4
10^3
150
400
800
1800
euop
incD mRNA
10^4
10^3
150
400
800
1800
hctBp
D
incV mRNA
10^4
10^3
175
300
600
1200
2400
euop
incV mRNA
10^3
100
400600
1200
hctBp

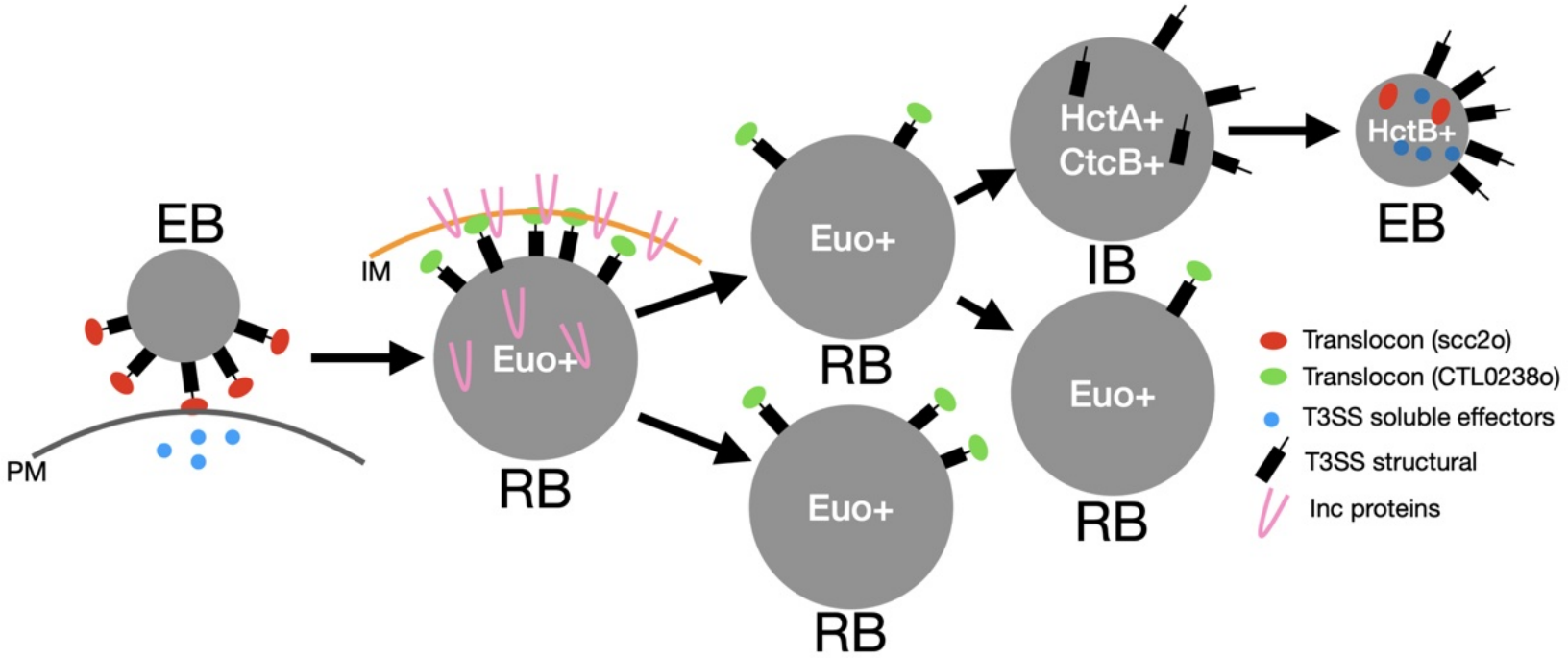
EB
PM
IM
Euo+
RB
Euo+
RB
Euo+
RB
HctA+
CtcB+
IB
Euo+
RB
HctB+
EB
Translocon (scc2o)
Translocon (CTL0238o)
T3SS soluble effectors
T3SS structural
Inc proteins